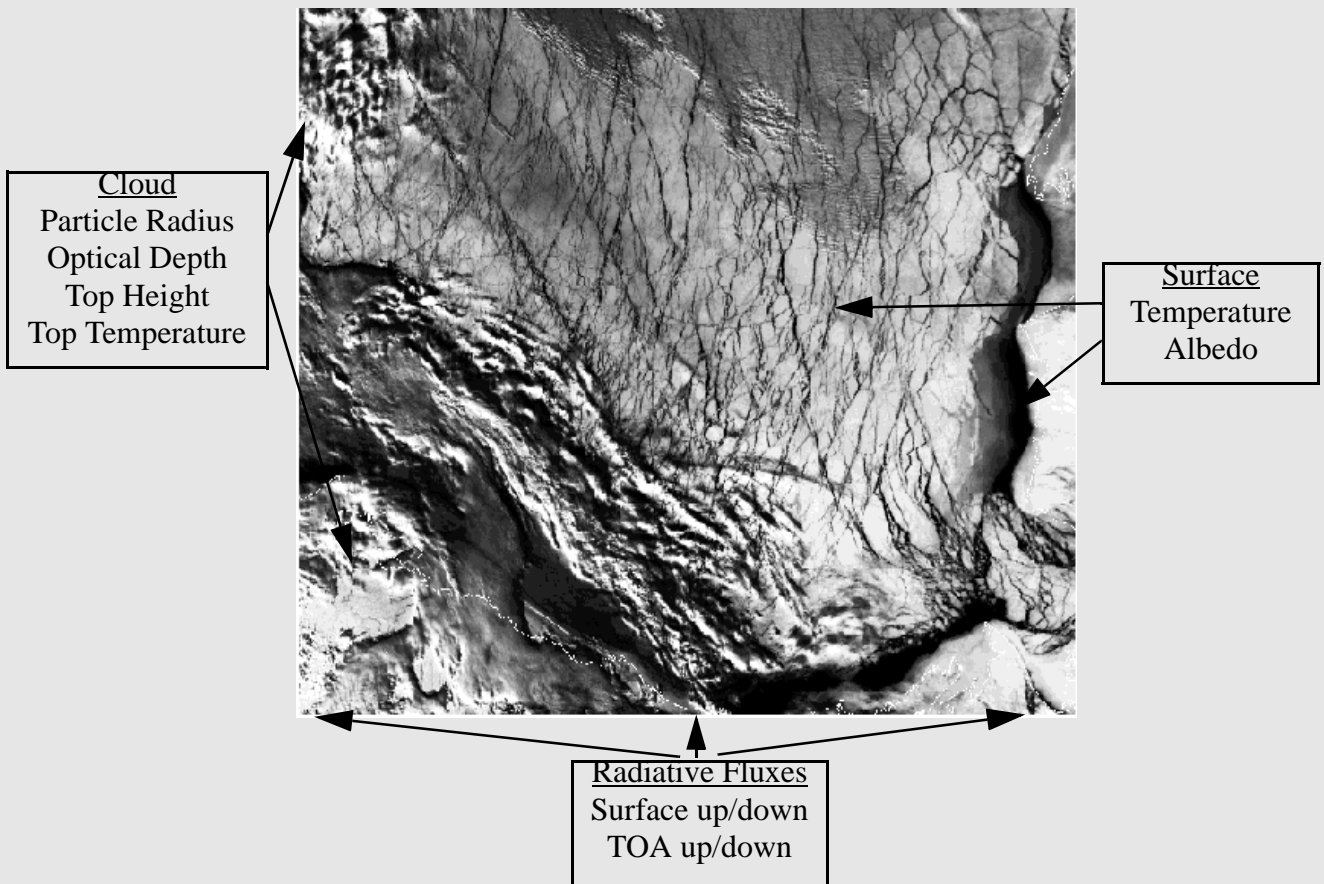


# The Cloud and Surface Parameter Retrieval (CASPR) System for Polar AVHRR

## USER'S GUIDE

Version 4.0

Beaufort Sea, AVHRR Channel 2



# The Cloud and Surface Parameter Retrieval (CASPR) System for Polar AVHRR

## USER'S GUIDE

Jeffrey R. Key

NOAA/NESDIS/ORA/ARAD/ASPT  
Madison, WI

January 31, 2002

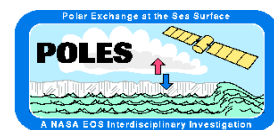


## TABLE OF CONTENTS FOR PART I

INTRODUCTION .....	2
Special Requirements.....	2
What CASPR Does Not Do .....	3
A Cautionary Note .....	3
What's New.....	3
Questions?.....	4
Acknowledgments.....	4
Referencing CASPR in Publications.....	4
Disclaimer .....	4
About the User's Guide.....	5
INSTALLATION.....	6
Obtaining CASPR .....	6
Installing CASPR.....	6
OPERATION.....	8
Overview .....	8
Running CASPR .....	10
The CASPR Help System .....	11
FILE INPUT AND OUTPUT .....	13
THE MAIN PROCEDURE: CASPR.....	17
Input Parameters and Keywords .....	17
The Widget Interface: wcaspr .....	25
DISPLAY OUTPUT .....	26
Displaying Results During caspr Execution .....	26
Displaying Results After the Fact: Individual Procedure Calls .....	27
Displaying Results After the Fact: The Procedure wplot.....	27
PROGRAM STRUCTURE .....	28
Common Blocks and Global Variables.....	28
Procedures .....	31
User-Modifiable Procedures .....	32
Batch Files.....	32

## TABLE OF CONTENTS FOR PART II

PROCESSING OVERVIEW.....	34
CONVERSION OF AVHRR CHANNEL INFORMATION.....	35
SURFACE PROPERTIES .....	36
Surface Temperature .....	36
Surface Albedo.....	37
WATER VAPOR.....	42
CLEAR SKY COMPOSITES .....	43
CLOUD PROPERTIES.....	44
Radiative Transfer Model .....	44
Cloud Detection .....	44
Cloud Particle Phase .....	53
Cloud Optical Depth and Particle Effective Radius.....	56

Cloud Water Path .....	58
Cloud Temperature and Pressure .....	61
RADIATIVE FLUXES .....	63
REFERENCES .....	65
REVISION HISTORY.....	68

---

---

# PART I: USAGE

---

---

Part I of the *CASPR User's Guide* describes how to use CASPR: downloading, installation, inputs/outputs, and execution. Refer to Part II for descriptions of the parameter retrieval algorithms.

# 1. INTRODUCTION

---

**C**ASPR is a toolkit for the analysis of data from the Advanced Very High Resolution Radiometer (AVHRR) satellite sensor carried on NOAA polar-orbiting satellites. The toolkit is a collection of algorithms that can be used to retrieve a variety of surface and cloud parameters. These algorithms are integrated into a user-friendly, flexible environment that includes on-line help and a multitude of options for displaying and printing results. CASPR can compute any or all of the following:

- Surface temperature, clear or all-sky
- Broadband albedo, clear or all-sky
- Cloud particle effective radius
- Cloud optical depth
- Cloud particle phase
- Cloud mask
- Cloud top temperature
- Cloud top pressure
- Precipitable water
- Downwelling shortwave radiation at the surface
- Downwelling longwave radiation at the surface
- Upwelling shortwave radiation at the surface
- Upwelling longwave radiation at the surface
- Downwelling shortwave radiation at the top of the atmosphere
- Upwelling shortwave radiation at the top of the atmosphere
- Upwelling longwave radiation at the top of the atmosphere
- Shortwave and longwave cloud radiative effect ("forcing") at the surface

CASPR also contains procedures for the display and manipulation of results, and for validation with user-supplied *in situ* data. Any number of images (e.g., a time series) can be processed.

## SPECIAL REQUIREMENTS

CASPR is written in the Interactive Data Language (IDL), a scientific visualization and data manipulation language from Research Systems, Inc. of Boulder, Colorado. Therefore, **IDL is required to run CASPR**. IDL is a commercial product; it is not freeware or shareware. Currently CASPR only runs under the UNIX operating system. A C compiler that can create shared libraries is also required.

All five channels of the AVHRR are required, as are images of solar zenith angle, sensor scan or zenith angle, and sun-sensor azimuth angle. Also needed are latitude/longitude images and a land mask. Processing can only be done for NOAA polar orbiters that have AVHRR channel 5: NOAA 7, 9, 11, 12, 14, 15, and 16. The input image data must be in a specific format (see *File Input and Output*).

The minimum amount of memory (MB) needed to compute all parameters is approximately:

$$[(ncols \times nrows \times 4 \times 34) + (npcols \times nprows \times nlevs \times 4 \times 3.5)]/1024^2 + 2$$

where *ncols* and *nrows* are the numbers of columns and rows in the image, *npcols* and *nprows* are the numbers of columns and rows in the profiles image, and *nlevs* is the number of profile levels. These requirements are for single-image cloud masking. For time series masking add

$$\{[ncols \times nrows \times 4 \times (ndays+1) \times 7.5] + (ncols \times nrows \times 4 \times 6)\}/1024^2$$

For example, given a 512 x 512 pixel image and an 8 x 8 cell profile image with 15 levels, about 36 MB of memory are needed if single-image cloud masking is employed. For time series masking using 5-day statistics add 51 MB for a total of 87 MB. If clear sky compositing is done (and it will be done with time series processing), add

$$(ncols \times nrows \times 4 \times 25 + ncols \times nrows \times 10)/1024^2,$$

e.g., 27.5 MB for a 512 x 512 pixel image. Clearly, times series masking with images larger than 512 x 512 pixels will require more memory than many workstations have. However, time series cloud masking can be run alone and then the resulting cloud masks can be read in when other parameters (surface and cloud properties and radiative fluxes) are to be computed. In that case the memory requirements would be the same as for single-image masking.

Temperature and humidity profiles and surface wind speed are required for the computation of cloud pressure.

## WHAT CASPR DOES Not Do

- Retrieval of temperature and humidity profiles (they must be input).
- Calibration of AVHRR raw data.
- Navigation and registration of raw data.
- Retrievals of some parameters for solar zenith angles between 80 and 89 degrees.
- Retrievals outside of the polar regions, although the primary limitation is the surface temperature retrieval, which could easily be expanded to include lower latitude oceans and land.
- Stratospheric clouds. All clouds are restricted to the troposphere.

## A CAUTIONARY NOTE

**CASPR is research code.** It does a lot of things well but doesn't do anything perfectly. Many of the algorithms have been validated, some have not. They are all detailed in the *Reference Guide*. There are three broad problems worth mentioning at the outset. First, everything depends on cloud detection, which sometimes borders on being as much an art as a science when working in the polar regions with the AVHRR. We are, indeed, trying to squeeze water from a stone. We do not claim to have solved the cloud detection problem, but rather provide methods that work reasonably well most of the time. Second, there are fundamental difficulties in estimating some parameters at extreme viewing and illumination geometries common to the high latitudes. We're venturing into territory that is difficult to model so beware. Third, the retrieval of cloudy sky parameters requires temperature and reflectance values underneath the clouds. CASPR interpolates clear sky values to cloudy areas. This generally works but can result in large uncertainties in very cloudy areas. Cautionary notes are given throughout the *Reference Guide*. Please do not ignore them!

## WHAT'S NEW

Version 4.0 has many significant changes. Surface cloud forcing parameters were added, NOAA-16 AVHRR/3 capabilities were completed, a new version of FluxNet was incorporated, the cloud detection procedures were revised, netCDF input and output file format support was added, daytime cloud particle

phase procedures were revised, a clear sky compositing strategy was added, support for providing a full surface type mask was added, and plotting procedures were enhanced. See *Revision History* in the *Reference* section for a longer list and see the revision history on the web site for a complete list of changes.

## QUESTIONS?

If you have questions or bug reports, contact:

Jeff Key  
NOAA/NESDIS  
1225 W. Dayton Street  
Madison, WI 53706  
e-mail: [jkey@ssec.wisc.edu](mailto:jkey@ssec.wisc.edu)

Are you on the mailing list? If you have requested information via e-mail then you are. If not, and you plan to use CASPR, please register via the Web at <http://stratus.ssec.wisc.edu>.

Continued work on this program is largely unfunded. I'll be happy to answer questions about things that are not in the User's Guide, and will fix bugs in a reasonably short period of time. Keep in mind, however, that I may not be able to provide an immediate response.

## ACKNOWLEDGMENTS

This work was supported primarily by NASA, the "POLES" project in particular, and NSF. Thanks are due to Mark Rehder, Ross Swick, and Todd Hutchinson for programming support, John Collins for the modification of various procedures for use over land surfaces, Dan Slayback for work on cloud masking, Rongqian Yang for work on the original v3.0 surface albedo retrieval procedures, and Adeline Wong for developing the cloudy sky surface temperature algorithm. Xuanji Wang contributed many utility procedures and has tested CASPR extensively. Lou Smith provided the anisotropic reflectance data. Erik Olson made some important revisions to the single-image cloud detection procedure. David Fanning wrote the color bar procedure. Bill Bellon compiled the APP sample data set.

## REFERENCING CASPR IN PUBLICATIONS

CASPR is comprised of algorithms, some have been published, others have not. If you are presenting results obtained using CASPR, how do you reference it? The most complete way would be to reference the individual pieces as described in *Part II: Reference*. As an alternative you might simply use "Key (2001, and references therein)", using the reference to this User's Guide:

Key, J., 2002, The Cloud and Surface Parameter Retrieval (CASPR) System for Polar AVHRR User's Guide, Cooperative Institute for Meteorological Satellite Studies, University of Wisconsin, 1225 West Dayton St., Madison, WI 53562, 61 pp.

## DISCLAIMER

This program is distributed as "freeware". Except when otherwise stated in writing the program is pro-



vided "as is" without warranty of any kind, either expressed or implied, including, but not limited to, the implied warranties of merchantability and fitness for a particular purpose. The entire risk as to the quality and performance of the program is with you. In no event unless agreed to in writing will the author or any other party who may modify and/or redistribute the program be liable to you for damages, including any general, special, incidental or consequential damages arising out of the use or inability to use the program. This includes, but is not limited to, the loss of data or data being rendered inaccurate or losses sustained by you or third parties or a failure of the program to operate with any other programs.

## ABOUT THE USER'S GUIDE

The *User's Guide* is divided into two parts. Part I contains instructions for obtaining and running CASPR. Part II describes the geophysical retrieval algorithms. In this User's Guide the following type-faces and symbols have special meaning:

- *Italics* are used for variable names.
- **Boldface** is used for file names and procedure names.
- < > are used in syntax descriptions, indicating items whose actual values or names should replace the angle brackets and what is contained between them; e.g., <filename> should be replaced by an actual file name..
- “ ” indicate literal strings; e.g., “@cmake” means type the text within the quotes, but not the quotes themselves.
- | means “or” and separates selections; e.g. 1|2|3 means select the integer 1, 2, or 3.

## 2. INSTALLATION

---

### OBTAINING CASPR

CASPR may be obtained via anonymous ftp from **stratus.ssec.wisc.edu**. Make a directory for the CASPR subdirectories that will be obtained; e.g., **mkdir caspr**. Change to that directory. Then:

```
ftp stratus.ssec.wisc.edu
logon as anonymous with your email address as the password
bin
cd pub/caspr
get caspr.tar.gz
get test/casprtest.tar.gz (if you want the test images and profiles)
quit
```

Next you must uncompress and extract the tar file:

```
gzip -d caspr.tar.gz
tar xvf caspr.tar
```

If all goes well then you should have a number of subdirectories and you can delete the tar file.

If you downloaded the test images and profile data, then create a **test** subdirectory of the main **caspr** directory, move the **casprtest.tar.gz** file there, unzip and untar it, then delete the tar file.

### *This Manual*

A postscript version of this manual is in the directory **pub/caspr/docs (userman.ps)**. Algorithms for the retrieval of surface and cloud properties are detailed in Part II: Reference (**refman.ps**).

### INSTALLING CASPR

Installing CASPR involves two steps: setting environment variables and compiling those components written in C.

#### *Step 1: Set Up the Environment*

The following environment variables need to be set or modified: **CASPR\_DIR**, the location of the main CASPR directory, **IDL\_PATH**, the search path for IDL, and **SHL\_EXT**, the filename extension used for the shared object libraries of the C modules (see below). The location of the CASPR files must be added to the **IDL\_PATH** environment variables so that they can be used from any directory. In UNIX you can add the following to your **.cshrc** file:

```
source $HOME/caspr/progs/setenv_caspr
```

**setenv\_caspr** is a script that sets the environment variables appropriately. If your main CASPR direc-

tory is not `$HOME/caspr` then you need to modify the above statement appropriately and edit the `setenv_caspr` file.

Under Microsoft Windows 3.1 or 95 you can set the `IDL_PATH` environment variable in the `autoexec.bat` file. Also, set a `TEMP` environment variable to a directory that can be used for temporary files. For example:

```
SET CASPR_DIR=C:\CASPR\PROGS
SET IDL_PATH=+C:\IDL\LIB;C:\CASPR\PROGS
SET TEMP=C:\TEMP
```

modifying the path `C:\CASPR\PROGS` appropriately. Under Windows NT 4.0 you should add the `IDL_PATH` variable to your environment via the System icon (in Control Panel) rather than editing `autoexec.bat`. Under all Windows versions you could instead edit the IDL path via IDL's Preferences dialog box.

Input image files may be compressed with either the Unix `compress` utility or with `gzip`. If one of these is used, then it must be in your search path. No verification of this is done. Results files may be compressed, but only `gzip` will be used. MSDOS versions of both of these compression programs are available at the same ftp site as CASPR.

Note that when transferring image and results binary files between UNIX and DOS, bytes must be swapped. See Section 4 for a further discussion of byte swapping.

### *Step 2: Compile the C Code*

In a few cases it was not practical to write IDL code to operate on entire arrays (images). For speed considerations these procedures were written in C. IDL allows calls to external routines via the `call_external` procedure. This facility is widely used in CASPR. So, external functions must be compiled into shared object libraries before running CASPR. A makefile for major Unix operating systems is provided. See the file `README.C` in the `progs` directory for further information. To learn more about `call_external`, the IDL documentation chapter *Operating System Access* in IDL version 4 or the IDL *Advanced Development Guide* in version 5 give details for the major operating systems.

So to build the shared object libraries for the C functions, type `make` at the Unix prompt. The makefile will determine the correct filename extension for the shared object libraries; e.g., Sun Solaris produces shared object files with an "so" extension. The `SHL_EXT` environment variable described above should be set to this extension automatically in the Unix script `setenv_caspr`. For Windows, an extension of "dll" is assumed (`globals.pro`). The shared libraries are expected to be in `$CASPR_DIR/progs`.

## 3. OPERATION

---

### OVERVIEW

CASPR is comprised of procedures to read image data, compute cloud and surface properties, display the image data and results, and perform validation. A CASPR session or job generally consists of invoking a set of procedures from the IDL command line, although there are two widget interfaces that can be used in place of command line calls. There are four main top-level procedures:

<b>caspr</b>
<b>wcaspr</b>
<b>chelp</b>
<b>wplot</b>

The main routine is **caspr**. This procedure can be used to handle all input, processing, plotting, and output. It has a long list of arguments and optional keywords that are detailed in section 4. The procedure **wcaspr** is a widget interface to **caspr** and is also described in Section 5. **chelp** is the help system (described below), and **wplot** is a widget interface useful for graphical output of the results (see section 6).

There are a number of procedures that are called by **caspr** but can also be called from the command line. Before the parameters can be retrieved, an image has to be read and preprocessed. The procedures for performing these tasks are:

<b>ingest_image</b>	<i>Read and preprocess an image</i>
<b>read_avhrr</b>	<i>Read (only) image</i>
<b>normalize</b>	<i>Normalize channels 1, 2, and 3A by the solar zenith angle</i>
<b>esdist_correct</b>	<i>Correct channels 1 and 2 albedo for Earth-Sun distance</i>
<b>ch3reflectance</b>	<i>Compute the reflectance portion of channels 3</i>
<b>cloudmask_1</b>	<i>Cloud mask a single image</i>
<b>cloudmask_n</b>	<i>Cloud mask a time series of images</i>

The procedures that perform the geophysical parameter retrievals are:

<b>surftemp_clear</b>	<i>Clear sky surface temperature</i>
<b>surftemp_cloudy</b>	<i>Cloudy sky surface temperature</i>
<b>surfalb_clear</b>	<i>Clear sky surface broadband albedo</i>
<b>surfalb_cloudy</b>	<i>Cloudy sky surface broadband albedo</i>
<b>precip_water</b>	<i>Cloudy sky precipitable water</i>
<b>narr2bb_toa</b>	<i>TOA narrow to broadband conversion</i>
<b>anis_correct12</b>	<i>Anisotropic reflectance correction of TOA albedo</i>
<b>atmos_correct</b>	<i>Atmospheric correction of TOA albedo</i>
<b>cloudphase</b>	<i>Cloud particle phase</i>
<b>cloudretau</b>	<i>Cloud optical depth and particle effective radius</i>
<b>cloudtemp</b>	<i>Cloud top temperature</i>
<b>cloudpress</b>	<i>Cloud top pressure</i>
<b>cloudwp</b>	<i>Cloud water path</i>

After the images have been ingested and the geophysical parameters have been retrieved, you may at some later time wish to work with the results. The following procedures are available for reading, manipulating, and validating the computed data.

<b>read_results_image</b>	<i>Read previously computed results arrays</i>
<b>read_results_means</b>	<i>Read previously computed summary statistics</i>
<b>read_cmask</b>	<i>Read a previously computed cloud mask</i>
<b>rdpix_results</b>	<i>Interactively show results pixel by pixel</i>
<b>area_results</b>	<i>Compute statistics for a region in an image</i>
<b>nfile_area_results</b>	<i>Compute statistics for an image area in multiple files</i>
<b>validate</b>	<i>Compare area statistics to in situ observations</i>
<b>area_average_results</b>	<i>Compute mean values for an area</i>
<b>average_time</b>	<i>Compute means over time</i>

There are a number of utilities that aid in analyzing algorithms and results including:

<b>rdpix</b>	<i>An enhanced version of the IDL rdpix procedure</i>
<b>rdpix_area</b>	<i>Mean, std. dev. of interactively defined area</i>
<b>tveq</b>	<i>Display hitogram-equalized image</i>
<b>tveq3</b>	<i>Display hitogram-equalized image image composite</i>
<b>latline_sample</b>	<i>Sample along a line of latitude</i>
<b>lonline_sample</b>	<i>Sample along a line of longitude</i>
<b>julian_day</b>	<i>A more useful julian day function</i>
<b>calendar_date</b>	<i>A more useful calendar date function</i>
<b>solar_zenith</b>	<i>Compute the solar zenith angle for a location and time</i>
<b>gcdistance</b>	<i>Compute the great circle distance between two points</i>
<b>write_netcdf_*</b>	<i>Write the parameters, cloudmask, etc. in netCDF format</i>
<b>read_netcdf_*</b>	<i>Read the parameters, cloudmask, etc. in netCDF format</i>

All of the above procedures and more are described in the online help.

## RUNNING CASPR

Both the C and IDL code must first be compiled. Compiling the C code was described in the *Installation* section. Compile the IDL procedures with the batch file **cmake.pro**. Start IDL and type

```
IDL> @cmake
```

("IDL>" is the IDL prompt). This will compile all procedures, set up the data structures, and change the command line prompt. While the C libraries need to be compiled only once, the IDL code must be compiled every time you start a new IDL session.

Next, to use the CASPR system you have three basic choices:

1. run the main procedure **caspr**, which calls the input, retrieval, display, and output routines,
2. call the procedures individually, or
3. use the widget interface **wcaspr**.

You can run the **caspr** routine from the IDL command line (see Section 5 for details), but it will generally be easier to run it from a batch file. An example file, **run.pro** in the **test** subdirectory is an illustration of this. It can be edited and run as a batch file; i.e.,

```
IDL> @run
```

Alternately, the values of the arguments to **caspr** can be specified in a separate file as in the sample file **caspr.def**. Similar to running **caspr** from the command line, **wcaspr** provides a widget interface to **caspr**. Section 5 explains these methods in more detail.

If you prefer to handle input, parameter retrieval, plotting, and output step by step, you can call each procedure individually. The top-level procedures were listed in the previous section, and their calling mechanism is available via the on-line help system described below.

### TIP

Most of the individual procedures require and/or compute image information, either the input image or results images (arrays). These are often not passed in/out explicitly, but rather through common blocks. All common block variables are available at the top level. See the last section of this guide for variable names and descriptions.

Of course, before you can run anything, you need data. CASPR is rather particular about input file format. See the *File Input and Output* section for details on the expected input file formats.

CASPR can be run from any directory. The subdirectory **CMASK** will be created and will contain the cloud mask files as well as statistics files if time series cloud masking is used. Other output, including temporary files, will be in the current directory.

The batch file **cexit.pro** can be run from the IDL prompt (@cexit) to delete variables (thereby freeing memory) and restore the "IDL>" prompt although you will probably never need to do this.

### TIP

Test images are available for download. You are strongly encouraged to experiment with these to better acquaint yourself with the system. Additionally, there is a simple tour that presents CASPR's major features and widget interfaces. To run the tour, type **tour** at the prompt.

## THE CASPR HELP SYSTEM

The CASPR help system contains information on algorithms, procedures, input, and output. It is invoked via

```
caspr> chelp
```

or by using the keyword **/help** when running **caspr**. A widget similar to the one in Figure 1 is then displayed.

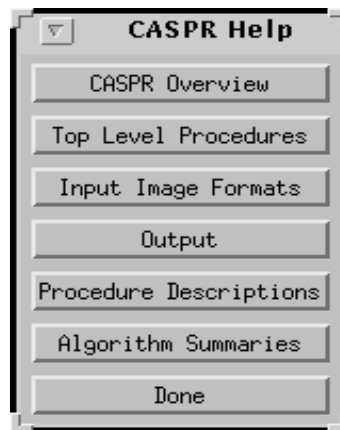


Figure 1. Top-level help widget.

Additional widgets are displayed when any of these buttons are selected. For example, selecting (clicking the left mouse button) the “Procedure Descriptions” gives the widget shown in Figure 2; selecting the “Output” button displays the widget in Figure 3.

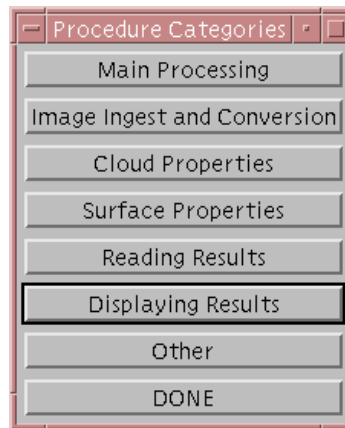


Figure 2. The Procedure Categories widget.

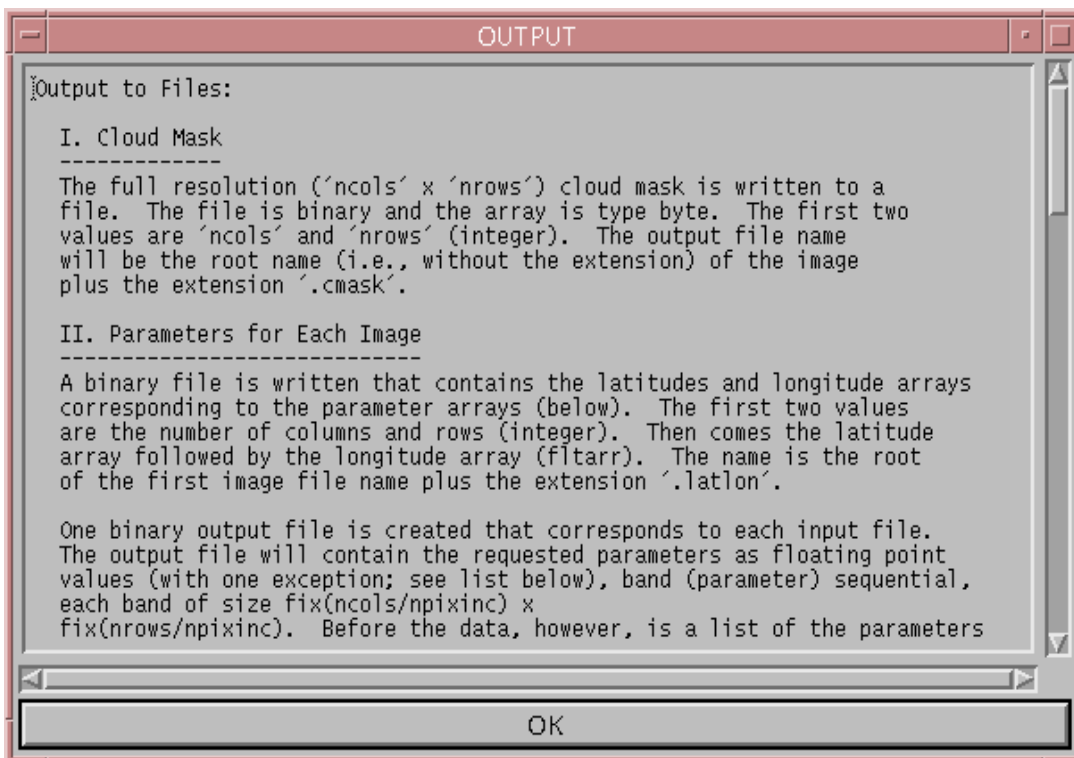


Figure 3. A help text widget example.



## 4. FILE INPUT AND OUTPUT

---

### *AVHRR*

The format of the input images is very specific. Each image file contains all five channels plus sensor scan, zenith or elevation angle, solar zenith angle, and the satellite-sun relative azimuth angle. Images are *ncols* samples by *nrows* lines, short (2-byte) integer. Data are band sequential with 8 bands:

- Channel 1, % albedo times 10 [0..1000]
- Channel 2, % albedo times 10 [0..1000]
- Channel 3, brightness temperature in Kelvin times 10. Starting with NOAA-16 it should be brightness temperature for channel 3B and % albedo times 10 [0..1000] for channel 3A.
- Channel 4, brightness temperature in Kelvin times 10
- Channel 5, brightness temperature in Kelvin times 10
- Satellite sensor scan, zenith, or elevation angle, degrees times 10
- Solar zenith angle, degrees times 10
- Relative satellite-sun azimuth, degrees times 10, where 180 is looking into the sun and 0 is looking away. Range: 0 to 180. (This is the opposite of the *Streamer* convention.)

All channels are expected to be calibrated. Note that the calibration scheme described in the NOAA Polar Orbiter's User Guide is generally not adequate for channels 1 and 2 because these channels degrade over time. See the *Reference Guide* for more information. If the image data were written on a computer with a different byte order than the one that will process the data, the the byte order must be reversed with the **caspr** keyword *swap\_bytes*. For example, if the data were calibrated, navigated, and put into the CASPR format on a Sun Sparc workstation but will be processed on a Linux PC (Intel), use *swap\_bytes*.

The input image files (AVHRR channels, latitude/longitude, and the land mask) may be compressed with either the standard UNIX 'compress' utility or with 'gzip'. If so, the ".Z" extension is required for 'compress' and the ".gz" extension is expected for 'gzip'.

If only a portion of your images is to be processed, either as a subregion or a subsampled (e.g., every third pixel) image, then the procedure **write\_subset** can be used to create the new file(s). See the file **subset.pro** or the online help for more information. CASPR operates on the entire image that it is given.

You can write a procedure to input the image data in other ways. The procedure **readusr\_avhrr** is available for this purpose. See the documentation in the file **usrimg.pro**.

### *Latitude/Longitude*

One latitude and one longitude image must be specified, so in the multiple AVHRR image case the data are assumed to be gridded. Latitudes and longitudes must be short (2-byte) integers with values as degrees times 100. Latitudes are positive north of the equator and negative for the Southern Hemisphere (0 to +-90 degrees, but times 100). Longitudes are positive east of the Prime Meridian and negative to the west (0 to +-180 degrees, but times 100). The lat/lon image arrays can be in the same file, in which case latitude comes first, or they can be in two different files.

## *Land Mask*

If both land and ocean areas are contained in an image, a land mask is required. If not, then the surface type (land or ocean) can be specified in place of the land mask filename. If there is a land mask, it is a byte array, corresponding in size and location to all AVHRR images to be processed. Either of two sets of values are required: 0=not-land and 254=land or 254=land, 0=open ocean, 3=sea ice, and 4=snow-covered land. If the latter set of values is given in the land mask, then set the **caspr** keyword *full\_landmask*. These can be changed by editing the variables NOTLAND, LAND, OCEAN, ICE, and SNOW in **globals.pro**. If only land and not-land are given, CASPR will further divide LAND into snow-free and snow-covered land, and NOTLAND into open water and sea ice. Note that SNOW means snow on land, not snow on ice, and ICE means sea ice, not land ice. The landmask is required for proper operation of the cloud mask, surface temperature, and surface radiative flux procedures.

## *Atmospheric Data*

If cloud top pressure is desired then the user must provide temperature (Kelvin), humidity (relative humidity, %), and pressure (mb) profiles. For the cloudy sky surface temperature, surface wind speed is required. These must ultimately be grids, with the lat/lon grid coordinates determined by **caspr** using the *profinc* and *pixsize* keywords (see **prof\_latlon** in **progrid.pro**). A variable number of profile levels over the grid is allowed. In the best case (computationally), your temperature, humidity, and wind data will be in the same lat/lon grid, though this is not required. Either way, you will need to modify the procedure(s) in **usrprof.pro** to read in your data. If wind speed is not available it should be set to MISSING in **usrprof.pro**, and the *cloudy* sky surface temperature will not be calculated. If profiles are available then they will be used to compute total precipitable water, which is used in albedo and radiative flux computations.

Total column ozone ( $\text{g/m}^2$ ), and aerosol visible optical depth (unitless) are always required, except in the case where only the cloud mask is being computed. An ozone image corresponding in size to the AVHRR imagery must be read or otherwise created. Aerosol optical depth is a single value that applies to the entire image area. Values for these parameters will probably be in data files, but exactly how these are stored and retrieved are controlled by the user. The procedures to change are **geto3** and **getaer**, also in **usrprof.pro**.

## *Clear Sky Composites*

This file is optional. It can be created by the user or generated automatically. It is used via the *clear\_composite* keyword to **caspr**. Its purpose is to store clear sky values for AVHRR channels 2 and 4, the surface temperature, and the broadband surface albedo as well as the cloud mask and the "bad" pixel arrays for the five most recent images. It only makes sense to use this in processing a time series of images, and it is recommended in that context. See the *Clear Sky Composite* section in the *Reference Guide*. This is a binary file with the following contents: the number of valid images for which clear values have been determined and stored in the subsequent arrays (1..5) [short integer], then three-dimensional floating point arrays dimensioned as (*ncols* x *nrows* x 5) containing clear values for AVHRR channel 2 reflectance (0..1), channel 4 (K), broadband surface albedo (0..1), surface temperature (K), precipitable water (cm), and byte arrays of the cloud mask and "bad" pixels (0 or 1). While it would be possible to create this file, it is not recommended. Simply set the *clear\_composite* keyword to a file name and let the program do the rest.

## *Surface Temperature Estimate*

This file is optional. Cloud detection at night can be improved with an estimate of the surface temper-

ature. If one is available and specified by the *tsurfest* keyword, it will be read as a floating point array *ncols* x *nrows* in size. The values must be in degrees Kelvin. Missing values must be set to MISSING. This file is only used in single image (not time series) cloud detection, as described in the *Reference Guide*. If clear sky compositing is being done, a clear sky surface temperature estimate will be automatically written to a file. The file can be used to aid cloud detection with the *tsurfest* keyword.

### ***Standard Output Files***

The **caspr** procedure outputs a variety of information to files. This output includes the cloud mask and computed parameters. Output file names use the root of the input image file name and then add an extension. The “root” is the file name less the extension, or less the last extension if there is more than one. When a time series or group of images is being processed, there are some output files that apply to all of them, e.g., the latitude/longitude images, the image mean parameters, etc. The names of these files will be the root of the first image name in the group, with the appropriate extension as detailed below. These files are output by the **caspr** procedure. If you are calling the individual parameter retrieval procedures yourself, you will also need to call the output routines in **results.pro**, as desired. Procedures are also available for writing and reading results in netCDF format. See the utilities section of the online help.

### ***Array Sizes***

A text file is written with the output parameter and array size information as well as the CASPR version number. The name of the file is the root of the first (and possibly only) image file name plus the extension **.sizes**.

### ***Cloud Mask***

The cloud mask is written to a separate file. The file is binary and the array is type byte. The first two values are *ncols* and *nrows* (integer). The output file name will be the root of the image’s name plus the extension **.cmask**. The file **globals.pro** contains definitions of the variables CLOUD, CLEAR, and BAD, which are used in the cloud mask.

### ***Parameter Results for Each Image***

One binary output file is created that corresponds to each input file. First is a list of the parameters that the file contains. The values are: 1=the parameter is present, 0=not present, as a 18-element short integer array. The parameters are given in Table 1 (page 23). Next are two short integer values: *ncols* and *nrows*, which are the size of the data arrays that follow. Then come the requested parameters as short integer (2-byte) arrays, except for the cloud phase and the refined surface type mask which are byte arrays. Output images are band (parameter) sequential. Units for all values are listed in Table 1. Clear pixels in cloud parameter arrays and cloudy pixels in clear arrays are generally MISSING, but that is not guaranteed. MISSING is also used for any invalid pixel. MISSING values should, of course, be ignored. If no clear sky pixels are found for one or more surface types in the image, all results are set to MISSING. No cloud or flux calculations are done for solar zenith angles between DARKZEN (85 degrees) and 90 degrees, so the corresponding pixels values are MISSING. The value for MISSING is 9999.0.

If either fluxes or cloud top properties were requested then the number of profile levels (integer) will be written, followed by the mean temperature, humidity, and pressure profiles (fltarr), each having that many levels. The output file name will be the root of the image name plus the extension **.params**.

### *Mean Parameter Values*

Another file is created with the mean value of each parameter. This is a text file with the date, parameter mean values, and parameter standard deviations for each of the standard parameters (Table 1) plus cloud amount. If more than one image was processed then data from all images is present.

The file is structured as follows. The first record is the list of binary values corresponding to each parameter, 1 if computed, 0 if not. The second record is the number of cases (equals the number of images processed) that the file will contain. The third record contains the mean values of the parameters (19 total). The fourth record will contain the standard deviations for all parameters. The records for the means and standard deviations will have values for every parameter, but those that were not computed will have values of MISSING. This includes the situation where no clear sky pixels were found for one or more of the surface types present. The file name is the root of the first image's name plus the extension **.means**. An example is:

```
1 1 1 1 1 1 1 1 1 1 1 1 1 1 1 1 1 1 1 1 1
 263
1992 6 29 21.88
 272.999  0.379594  16.0942  4.33651  1.11329  262.619
 652.282  1.84806  38.2547  613.432  277.001  220.099
 316.748  715.730  314.146  227.239  -40.593  32.714  0.602507
...
```

## 5. THE MAIN PROCEDURE: CASPR

---

The calls to the main procedure, **caspr**, and its widget counterpart, **wcaspr**, have the following syntax:

```
caspr, fln, latlonfln, landfln, ncols, nrows, parameters, /multiimage, /multiland,  
/swap_bytes, /user_image_format, /esdist, lookang=1|2|3, /norm, cmask_type=0|1|2,  
threshadj=<num>, rethresh=1|2|3, ndays=<num>, cellrad=<num>, profinc=<num>,  
pixsize=<num>, /full_landmask, clear_composite=<string>, tsurfest=<string>,  
image_dir=<string>, profile_dir=<string>, latlon_dir=<string>, land_dir=<string>,  
/compress_results, display=<string-list>,  
/no_output, /pause, /log, /no_warn
```

```
caspr, /help
```

```
caspr, argfile=<filename>
```

```
wcaspr
```

```
wcaspr, argfile=<filename>
```

### INPUT PARAMETERS AND KEYWORDS

#### Required Arguments:

*fln*

The "file name" of the AVHRR image or, if the keyword *multiimage* is set, then a filename or filenames of the AVHRR images to be processed. If *multiimage* is not used, then this "file name" is a string that contains first the file name, then the 2- or 4-digit year, month, day, GMT hour and minutes in the form <hhmm>, and the NOAA satellite number (e.g., 7, 9, 11, 12, 14, 15, 16). All MUST be separated by commas. Spaces are ignored. For example, a valid file name is:

```
file1.img,92,4,18,2345,11
```

This is also the format that must be used for the "file names" in the file *fln* if the keyword *multiple* is used. If the file name ends in ".Z", it is assumed to be compressed and will be uncompressed before reading and recompressed after. For time series processing the file names are expected to be in chronological order; e.g., day 1 then day 2, etc.

If *fln* is a file containing "file names" then it must be in either the current directory or the image directory (below). Therefore, *fln* must not include the path specification. Note: If the year is 2-digit, then values of 50 or more are 19xx; values less than 50 are 20xx.

See *File Input and Output* for details on file structure.

*latlonfnn* The name of the file containing the latitude and longitude data corresponding to the image or an array of two file names if latitudes and longitudes are in separate files. In either case, latitude comes first. *latlonfnn* is assumed to be in the current directory or in *image\_dir* unless *latlon\_dir* is set. It must not include the path. See *File Input and Output* for details on file structure.

*landfnn* The file name of the landmask. *landfnn* is assumed to be in the current directory or *image\_dir* unless *land\_dir* is set. It must not include the path. If no landmask is available, and if the surface type is uniform throughout the image, specify either 'LAND' or 'OCEAN' (uppercase or lowercase, as strings) for *landfnn*. If there is a landmask file, it cannot be named 'LAND' or 'OCEAN'. See *File Input and Output* for details on file structure. See also the *full\_landmask* keyword.

*ncols, nrows* The number of columns (pixels across) and rows of pixels in the AVHRR imagery.

*parameters* This is a string indicating which parameter group is to be computed. Possible values are:

'cmask'  
'clear'  
'cloud'  
'flux'

which represent the cloud mask ONLY; clear parameters: surface temperature and broadband albedo, precipitable water; cloudy parameters: all-sky surface albedo and temperature, cloud particle effective radius and optical depth, cloud top temperature and pressure, plus all clear sky parameters; surface radiative fluxes plus all clear and cloudy parameters. Atmospheric temperature and humidity profiles are required for cloud pressure. If they are not provided (*profinc* = -1, below), cloud pressure will not be computed.

Table 1 lists the possible output parameters and Table 2 shows which of these the various *parameters* strings produces. Note that 'cloud' includes 'clear' and both of the flux groups include cloud parameters.

**Optional Keywords:**

*multiimage* Set this keyword (*/multiimage*) if more than one AVHRR image is to be processed. If it is set, then *fnn* is the name of a file containing the names of all the AVHRR image files. See the description of *fnn* for the special "file name" format to be used.

*multiland* Set this keyword (*/multiland*) if more than one AVHRR image is to be processed (*/multiimage*) and you will provide a different land mask (surface type image) for each. If it is set, then *landfnn* is the name of a file containing the names of all the land masks.

<i>swap_bytes</i>	Set this keyword ( <i>/swap_bytes</i> ) if the byte order of the binary image files (AVHRR and lat/lon) should be switched. This is necessary when images created on a UNIX machine are being analyzed on a PC or vice versa. It may also be needed on DEC systems.
<i>user_image_format</i>	How will the AVHRR image data (except the lat/lon data and the land mask) be input? If this keyword is not present then the standard format and internal procedures will be used. If this keyword is set (" <i>/user_image_format</i> ") then the user-modified procedure <b>readusr_avhrr</b> (in <b>usrimg.pro</b> ) will be used to read in the image data.
<i>esdist</i>	Set this keyword if the channels 1 and 2 data are input as albedos and should be adjusted for variations in Earth-Sun distance (date dependent). Note: The standard NOAA calibration procedure does <b>not</b> adjust for Earth-Sun distance variations.
<i>lookang=1 2 3</i>	The type of sensor look angle, where 1=scan angle, 2=satellite zenith angle, 3=satellite elevation angle. Default=1.
<i>norm</i>	If set ( <i>/norm</i> ) then AVHRR channels 1, 2, and 3A (NOAA-16 and higher, sunlit portion only) are assumed not to be normalized by the cosine of the solar zenith angle and they will be normalized here. If not set then the channels 1, 2, and 3A albedos are assumed to be normalized.
<i>cmask_type=0 1 2</i>	This option controls the type of cloud masking to be done, where 0=no cloud masking, 1=single-image cloud masking, and 2=time series cloud masking. If no cloud masking is to be done, then the cloud mask will be read, and the assumed file name is the root of the image file name with the extension <b>cmask</b> (see Section 4). If <i>cmask_type=2</i> then cloud masking will be done on a time series of daily (same time of day) data, typically from 1-15 days. If <i>cmask_type=1</i> then each individual image is masked independently of the others. In general, masking individual images is not as accurate. The default is to compute the single-image cloud mask ( <i>cmask_type=1</i> ).
<i>threshadj=&lt;num&gt;</i>	The cloud masking threshold adjustment factor. If less than 100 then marginally cloudy pixels will be labeled as cloudy, so that those pixels labeled as clear are more likely to actually be clear; i.e., the algorithm is "clear-conservative". If greater than 100 then the algorithm is "cloud-conservative", meaning that those pixels labeled as cloud are more likely to be cloud. Values less than 100 will result in a higher cloud fraction; values greater than 100 will result in a lower cloud fraction. A reasonable range is 70 – 130%. The default is 100 (%).
<i>rethresh=1 2 3</i>	Use this keyword to perform an additional step in the single image cloud detection that rethresholds the clear part of the image based on the local mean clear sky brightness temperature. Otherwise, only spectral tests are used. Set <i>rethresh=1</i> for daytime rethresholding, <i>rethresh=2</i> for nighttime, and <i>rethresh=3</i> for both.

<i>ndays</i> =<num>	The number of days (images) to use in the time series cloud masking. Clear sky statistics will be gathered over <i>ndays</i> days and the cloud masking will then be done. While increasing the number of days will provide more clear sky statistics, the variance in the spectral features will increase so there is a tradeoff. The default number of days is 5. This keyword is only used if <i>cmask_type</i> =2.
<i>cellrad</i> =<num>	The "radius" of the cells for which clear statistics will be computed in the cloud masking procedures (time series or single image methods). A value of 20 implies 41x41 pixel cells. In the time series approach, <i>ndays</i> and <i>cellrad</i> together control how many clear values go into the clear sky statistics. Default: <i>75/pixsize</i> .
<i>profinc</i> =<num>	The distance in kilometers between temperature and humidity profiles (and ozone). <i>profinc</i> must correspond to the grid spacing in the user profile data. If only one profile is being used, set <i>profinc</i> to the maximum dimension (in km) of the imagery. Default=100 km. <b>Special case:</b> a value of -1 indicates that profiles are not available. In this case, cloud top pressure will not be computed or output.
<i>pixsize</i> =<num>	The AVHRR pixel size, typically either 1 km (LAC) or 4 km (GAC). If an image is subsampled then use the equivalent size. This is used to determine how often a profile is chosen. Default=1 km.
<i>full_landmask</i>	If set, this keyword indicates that the land mask that was read is "complete", i.e., that all surface types LAND, OCEAN, ICE, and SNOW are already defined with values as specified in <b>globals.pro</b> . In that case, the land mask will not be refined further. Otherwise, the landmask is expected to have values of LAND and NOTLAND, which may be relabelled as SNOW and ICE or OCEAN. If the land mask also has SNOW, ICE, or OCEAN values, they will be used as is. LAND means snow-free land (vegetation cover), OCEAN means open water, ICE means sea ice (with or without snow), and SNOW means snow-covered land.
<i>clear_composite</i> = <string>	Set this keyword to a file name that will hold the clear sky composite for various channels/parameters. If the file doesn't exist it will be created. If this keyword is set with <i>"/clear_composite"</i> , the default file name <i>'clearcomposite.img'</i> will be used. See <i>Input and Output Files</i> in this guide for details on file structure. The clear composite is used to fill cloudy pixels for parameters that are needed in cloudy sky retrievals. It can be used for both time series and single image processing, though it really only makes sense for a time series. See the <i>Reference Guide</i> for more information on compositing.
<i>tsurfest</i> =<string>	This keyword allows for the input of a surface temperature estimate that will be used in single image cloud detection. Set it to a file name, with the file structure as described in the <i>File Input and Output</i> section.



<i>no_output</i>	If this keyword is set ( <i>/no_output</i> ) then neither the cloud mask nor the parameter results files will be written. These results arrays, which are listed in Common Blocks and Global Variables ( <i>Program Structure</i> section), can be output as desired by the user. Note: If <i>no_output</i> is set, parameter means for time series plots will not be available.
<i>pause</i>	If this keyword is set ( <i>/pause</i> ) then the user is prompted to continue after each image in a sequence is processed. This is only valid when the <i>multiple</i> keyword is used.
<i>image_dir=&lt;string&gt;</i>	If present, then this keyword gives the directory location of the images, INCLUDING the lat/lon images and the land mask. If not present then all image files are assumed to be in the current directory.
<i>profile_dir=&lt;string&gt;</i>	If present, then this keyword gives the directory location of the profile data, including ozone data. It is passed to the user-modifiable procedures <b>getusrprof</b> , <b>geto3</b> , and <b>getaer</b> .
<i>latlon_dir=&lt;string&gt;</i>	If present, then this keyword gives the directory location of the lat/lon data.
<i>land_dir=&lt;string&gt;</i>	If present, then this keyword gives the directory location of the landmask (surface type) data.
<i>display=&lt;list&gt;</i>	Use this keyword if you want to see some of the retrieval results on the screen as the image files are processed. The list contains parameter and plot type identifiers, where each element is a string composed of the parameter number in the list (Table 1) and one of the characters 'i', 'm', 'h', or 't', for image plot, mapped image plot (on a map projection), relative frequency histogram, or time series plot, respectively (case insensitive).  In addition to the 16 standard parameters, there are three more that can be displayed. Parameter #19 is the cloud mask or cloud fraction (for time series plots), #20 is the AVHRR image, and #21 is the average temperature/humidity profile for the image (if available). None of these needs a plot type character.  Parameter #19 is unique in that the display value of '19' (no plot type) signifies that the cloud mask should be plotted, but '19t' means use the cloud fraction in a time series plot. No other plot type is valid for this parameter.  For example, "caspr,...,display=['1h','4i','12T','20']" displays a histogram of surface temperature, an image plot of cloud optical depth, a time series plot of the upwelling shortwave flux at the surface, and the satellite image.
<i>compress_results</i>	If this keyword is set then the <b>*.params</b> file(s) (see output section) and the cloud mask(s) will be compressed using <b>gzip</b> , which must be in your search path.
<i>log</i>	If set ( <i>/log</i> ) then all output messages are sent to the file CASPR.LOG as well as to the screen.

- help* Use this keyword with no other parameters (e.g., *caspr/help*) to access the help system. This is equivalent to calling **chelp**.
- no\_warn* Set this keyword (*/no\_warn*) to suppress warning messages.
- argfile=<filename>* The file name of a file containing the values of all arguments passed into the procedure **caspr**. For **wcaspr**, these values become the defaults which can then be changed via the widget interface. This file has a simple but specific format subject to these constraints:
- Comments are allowed AFTER the argument values on a line, and must be preceded by a semi-colon. They may not be continued on another line.
  - The argument values must be on the lines as shown in the file **caspr.def**; i.e., one parameter per line in the order shown in that file.
  - String variables must NOT have enclosing quotes.
  - Array elements must NOT have enclosing square brackets.
  - For multi-values arguments (arrays), elements must be separated by a comma. Spaces are ignored.
  - The first line in the file is a comment line and is ignored.
- This keyword should be used alone; e.g., *caspr,argfile='caspr.def'*.

Table 1. Output parameters, their integer reference numbers, and the symbols used in the text to represent them. The output factor is a multiplier. For example, surface temperature is stored as degrees Kelvin time 10, as an integer (intarr = 2 bytes, bytarr = 1 byte). See the *Common Blocks* section for variable names.

Reference Number	Description	Internal Units/Range	Output Factor and Type	Symbol
1	Surface temperature, clear or all-sky (sea ice only), depending on what was requested	K	x10, intarr	$T_s$
2	Broadband albedo, clear or all-sky, depending on what was requested <sup>1</sup>	Unitless, [0,1]	x1000, intarr	$\alpha_s$
3	Cloud particle effective radius	microns [water: 2.5-20; ice: 20-120]	x10, intarr	$R_e$
4	Cloud visible, vertical optical depth	Unitless [water: 0-150; ice: 0-50]	x10, intarr	$\tau_c$
5	Cloud particle phase	0=liquid, 1=ice	bytarr	$\phi_c$
6	Cloud top temperature	K	x10, intarr	$T_c$
7	Cloud top pressure	mb	x10, intarr	$P_c$
8	Precipitable water (clear sky if no profiles)	cm	x10, intarr	$PW$
9	Refined surface type mask	open ocean=0, snow-free land=254, snow=4, ice=3,	bytarr	$S_{type}$
10	Downwelling shortwave radiation, surface	$W m^{-2}$	x10, intarr	$SW\downarrow_{srf}$
11	Downwelling longwave radiation, surface	$W m^{-2}$	x10, intarr	$LW\downarrow_{srf}$
12	Upwelling shortwave radiation, surface	$W m^{-2}$	x10, intarr	$SW\uparrow_{srf}$
13	Upwelling longwave radiation, surface	$W m^{-2}$	x10, intarr	$LW\uparrow_{srf}$
14	Downwelling shortwave radiation, TOA	$W m^{-2}$	x10, intarr	$SW\downarrow_{toa}$
15	Upwelling shortwave radiation, TOA	$W m^{-2}$	x10, intarr	$SW\uparrow_{toa}$
16	Upwelling longwave radiation, TOA	$W m^{-2}$	x10, intarr	$LW\uparrow_{toa}$
17	Shortwave cloud forcing at the surface	$W m^{-2}$	x10, intarr	$CF_S$
18	Longwave cloud forcing at the surface	$W m^{-2}$	x10, intarr	$CF_L$

<sup>1</sup>See the *Reference Guide* for more information on the type of albedo produced.

Table 2. User-requestable parameters and the output parameters that they produce.

<i>params</i> String	Output Parameters
'cmask'	The cloud mask.
'clear'	$T_s \alpha_s PW S_{type}$
'cloud'	$T_s \alpha_s Re \tau_c \phi_c A_c T_c P_c PW S_{type}$
'flux'	$T_s \alpha_s Re \tau_c \phi_c A_c T_c P_c PW S_{type}$ $SW\downarrow_{srf} LW\downarrow_{srf} SW\uparrow_{srf} LW\uparrow_{srf} SW\downarrow_{toa} SW\uparrow_{toa} LW\uparrow_{toa} CF_S CF_L$

## THE WIDGET INTERFACE: WCASPR

The widget interface to **caspr** is **wcaspr**. When **wcaspr** is invoked, either alone or with the *argfile* keyword, the widget shown in Figure 4 appears. The user can then choose values for the input parameters and keywords in a point-and-click manner rather than typing them on the command line.

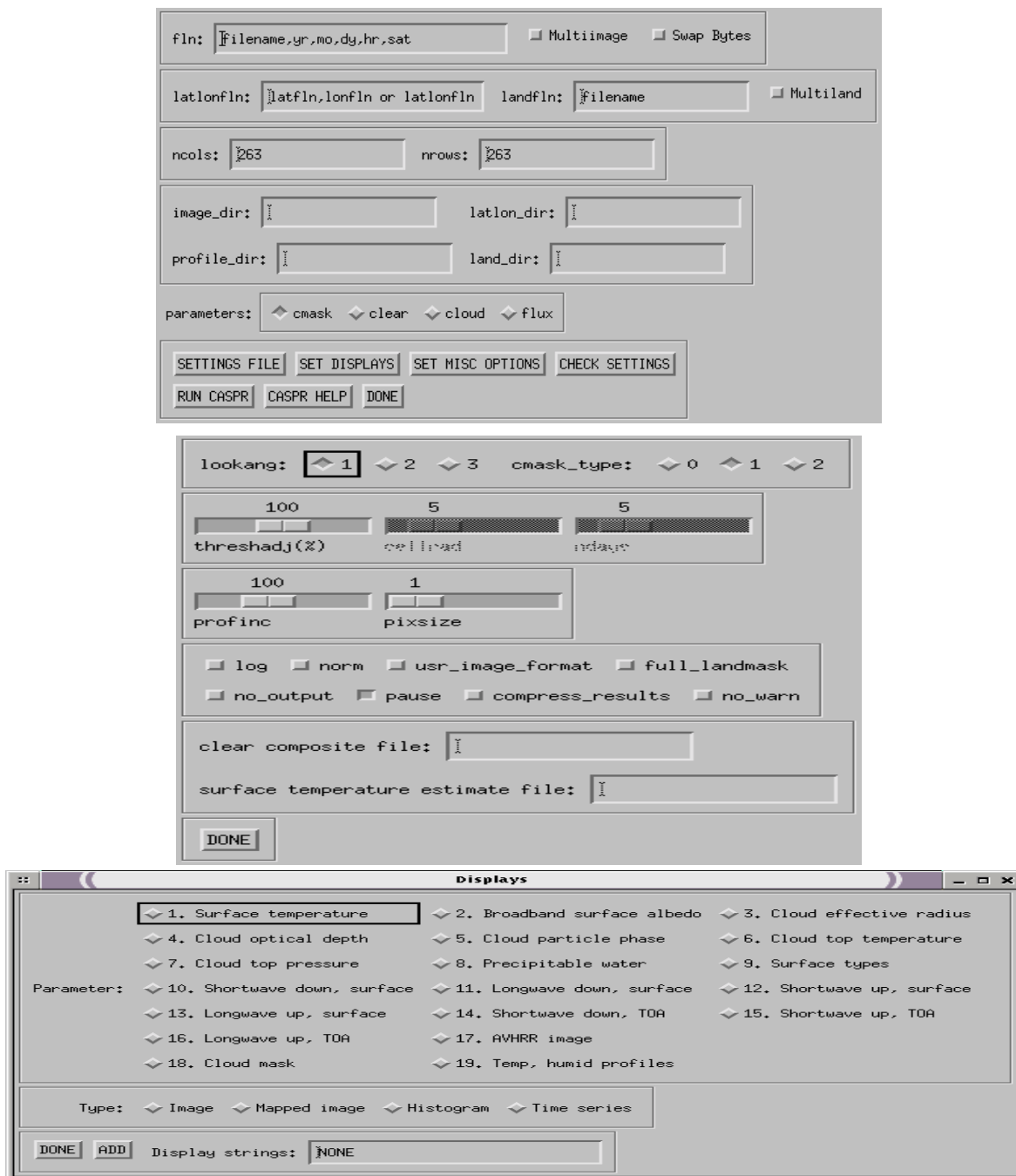


Figure 4. The main **wcaspr** widget and two of its subwidgets (middle and bottom) that are displayed when the “Set Displays” and “Misc Options” buttons are clicked.

## 6. DISPLAY OUTPUT

---

Results and image data can be displayed in a variety of ways. The “automatic” approach is to use the *display* option in the call to **caspr**. Examples of this approach are given in the next section. If you prefer to wait until after an image has been processed, either the widget plotting interface **wplot** can be used, or individual plotting procedures can be called. These are described in the second and third sections below.

### DISPLAYING RESULTS DURING CASPR EXECUTION

Resulting parameter arrays and/or the AVHRR image and cloud mask can be displayed while **caspr** is running by using the *display* keyword. For each parameter one of four different plot types can be specified: a histogram summarizing the values over the entire image, an image plot with color bar, a mapped image plot, or a time series plot (if a time series is being processed) of the results array. Examples are shown in Figure 5.

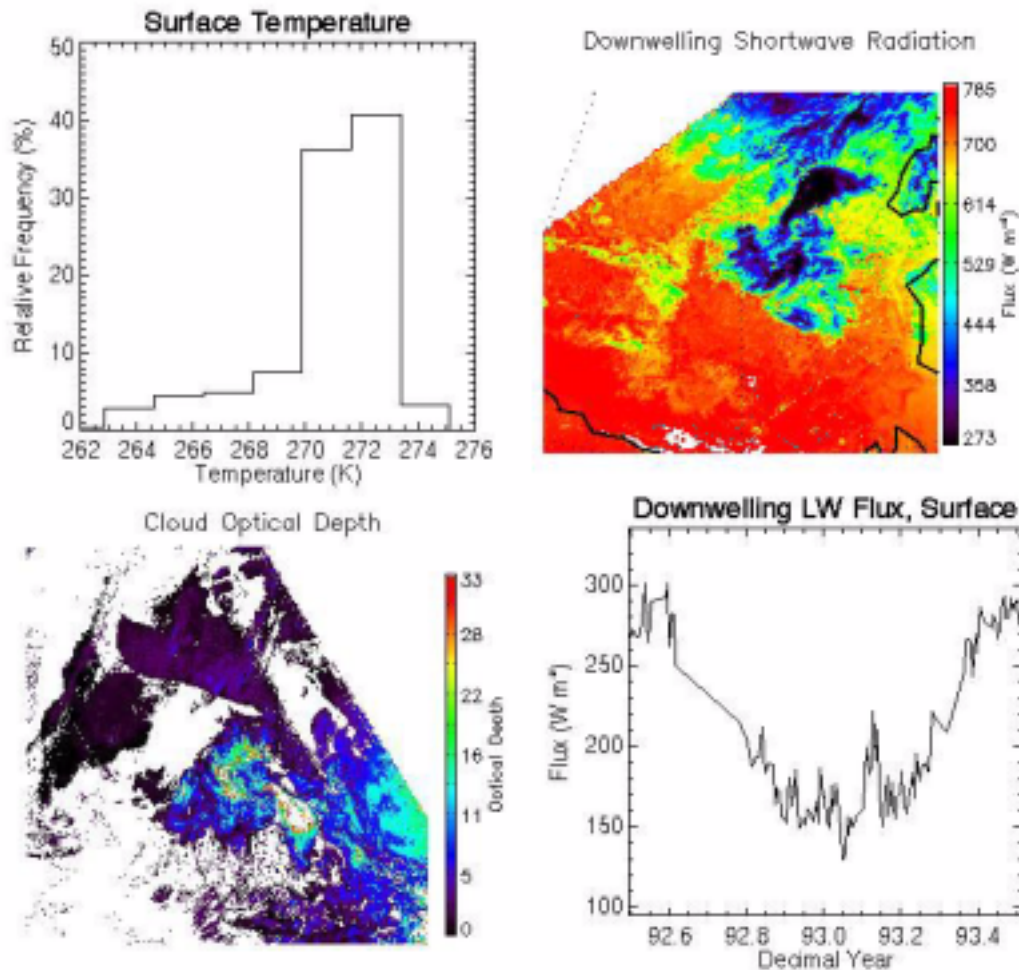


Figure 5. An example of the display and plot types available in CASPR for a single image (first three plots) and a year-long time series over the Beaufort Sea in June, 1992.

## DISPLAYING RESULTS AFTER THE FACT: INDIVIDUAL PROCEDURE CALLS

There are a variety of procedures that are employed for plotting and may be called by the user. In all cases the names of the variable arrays are passed in as arguments. The procedures are:

```
plot_profile
plot_image
plot_series
contlevels
tveq
tveq3
```

Those starting with “plot\_” do the actual plotting. Some of them require a contour/binsize interval, which can be computed with the procedure **contlevels**. For Postscript output to a file, you’ll have to either call the individual plot procedures or use **wplot**. For simple display of the raw arrays, whether a results array or an image channel, try **tveq,array,new**.

## DISPLAYING RESULTS AFTER THE FACT: THE PROCEDURE WPLOT

The procedure **wplot** (no arguments) can be used to plot results on a map projection and either display them on the screen or print them to a Postscript file. Up to four plots can be placed on a single page. This procedure has a widget interface, as shown in Figure 6.

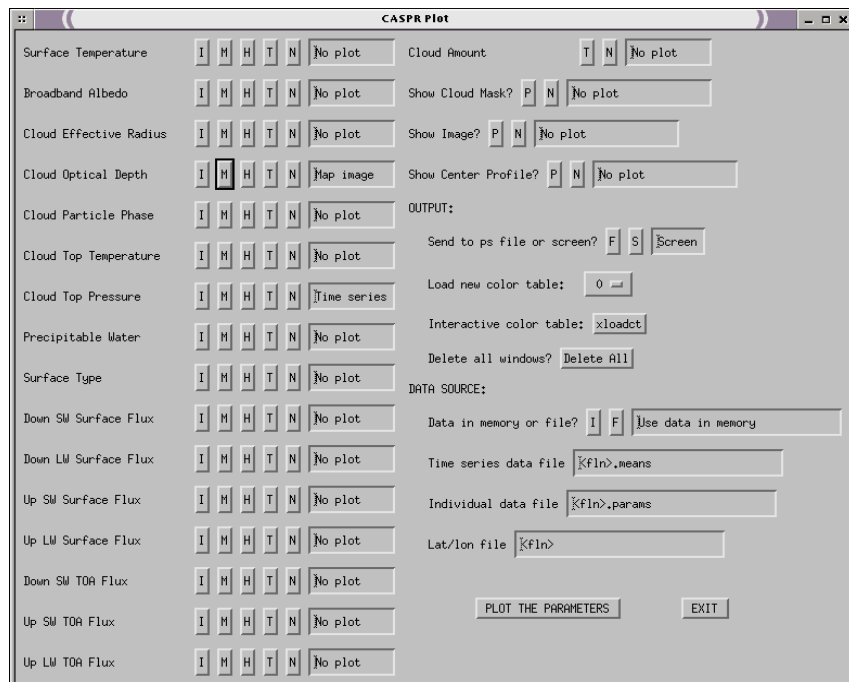


Figure 6. The plot-print widget used for final, publication-quality plotting.

## 7. PROGRAM STRUCTURE

---

### COMMON BLOCKS AND GLOBAL VARIABLES

The following common blocks are declared:

```

common avhrr,ch1,ch2,ch3,ch4,ch5,scan,solzen,relaz,ch3ref,igood,badpix
common avhrr_n,ch1n,ch3n,ch4n,ch5n,ch3refn,scann,solzenn,cmaskn,badpixn
common avhrr_latlon,lat,lon,landmask,landmask2
common profs,pcellsize,npcols,nprows,nplevs,ptemp,ph2o,pp,plat,plon,oz,hz,wind
common cldmask,cmask,iclr,icld
common results_srf,tsurf,broadalb,pw
common results_cld,cldre,cldtau,cldphase,cldtemp,cldpress
common results_fluxes,swdnsrf,swupsrf,lwdnsrf,lwupsrf,swdntoa,swuptoa,lwuptoa
common results_fluxes2,swcldfrc,lwcldfrc
common params,params_list,requests,outparams
common globals,MISSING,VERSION,MAXPARMS,MAX_SCREEN_PLOTS,DISPWIN
common globals2,CLEAR,CLOUDY,WATPHASE,ICEPHASE,BAD,LAND,NOTLAND,
OCEAN,ICE,SNOW
common globals3,OS,UNIX,DOS,SHL_EXT,SHL_DIR,CASPR_DIR,DIRCHAR,WFONT,WDEV
common globals4,DARKZEN
common globals5,DEBUG,NOWARNINGS
common globals6,TRUE,FALSE

```

These variables are available at the top level; e.g., at the IDL prompt. Of course, they will not actually be defined or have values until after **caspr** has been run. The following table gives a description of those variables that are likely to be of interest to the user.

CATEGORY	VARIABLE DESCRIPTION	ASSIGNED IN PROCEDURE
<b>IMAGE DATA</b>		
ch1, ch2	AVHRR channels 1 and 2, albedo in the range [0,1] [fltarr].	read_avhrr
ch3, ch4, ch5	AVHRR channels 3, 4, and 5 brightness temperatures [fltarr].	read_avhrr
scan	Sensor scan, zenith, or elevation angle, degrees [fltarr].	read_avhrr
solzen	Solar zenith angle, degrees [fltarr].	read_avhrr
relaz	Satellite-sun relative azimuth, detrees [fltarr].	read_avhrr
lat, lon	Latitude and longitude, degrees [fltarr].	read_latlon
NOTE: As described in Section 4, the above variables were input with multiplicative factors, e.g., temperature times 10. They were converted upon input.		
landmask	The land mask, where 0=ocean and 254=land [bytarr].	read_landmask
<b>DERIVED IMAGES</b>		
ch3ref	Channel 3 reflectance (%), in the range [0,1] and normalized for the solar zenith angle [fltarr].	ch3reflectance



landmask2	The refined landmask with values of LAND for snow-free land (vegetation), SNOW for snow-covered land, OCEAN for open water, and ICE for sea ice (with or without snow). [bytarr]	surftype
igood, badpix	The array indices (from ‘where’) of the valid pixels in the AVHRR imagery [lonarr], and the “image” of bad/invalid pixels where FALSE=good pixel and TRUE=bad.	check_avhrr

**PROFILES**

pcellsize	The size of each profile cell in pixels of the AVHRR imagery.	prof_latlon
npcols, nprows, nplevs	The number of columns, rows, and levels in the profile arrays.	prof_latlon
ptemp	Temperature profile (K) [fltarr].	profgrid
ph2o	Relative humidity profile (%) [fltarr].	profgrid
pp	Pressure profile (mb) [fltarr].	profgrid
plat, plon	Latitude and longitude (degrees) of the profile arrays [fltarr].	prof_latlon
oz	Total column ozone amount (Dobson units) [scalar].	o3aer
hz	Total column aerosol optical depth (unitless) [scalar].	o3aer
wind	Surface wind speed ( $m\ s^{-1}$ )	profgrid

**RESULTS**

cmask	The cloud mask image, with values of CLEAR, CLOUDY, and BAD, as defined below [bytarr].	cloudmask_1,
iclr, icld	Array indices of clear and cloud pixels in ‘cmask’ [lonarr].	cloudmask_n
landmask2	The landmask corresponding to the results arrays, where LAND is snow-free land, SNOW is snow-covered land, ICE is sea ice (snow-covered or snow-free), and OCEAN is open water (see <b>globals.pro</b> for actual values).	cloudmask_1,
tsurf	Surface temperature (K) [fltarr].	cloudmask_n
broadalb	Broadband surface albedo in the range [0,1] [fltarr].	retrieve
cldre	Cloud particle effective radius (microns) [fltarr].	surftemp_clear,
cldtau	Cloud optical depth (unitless) [fltarr].	surftemp_cloudy
cldphase	Cloud particle phase, 0=liquid, 1=solid (ice) [fltarr].	surfalb_clear,
cldtemp	Cloud top temperature (K) [fltarr].	surfalb_cloudy
cldpress	Cloud top pressure (mb) [fltarr].	cloudretau
pw	Precipitable water for the atmospheric column (cm) [fltarr].	cloudretau
vp	Near-surface vapor pressure (mb) [fltarr].	cloudphase
swdnsrf	Shortwave downwelling flux at the surface ( $W\ m^{-2}$ ) [fltarr].	cloudtemp
swupsrf	Shortwave upwelling flux at the surface ( $W\ m^{-2}$ ) [fltarr].	cloudpress
lwdnsrf	Longwave downwelling flux at the surface ( $W\ m^{-2}$ ) [fltarr].	precip_water
lwupsrf	Longwave upwelling flux at the surface ( $W\ m^{-2}$ ) [fltarr].	vapor_press

swdntoa	Shortwave downwelling flux at the top of the atmosphere ( $\text{W m}^{-2}$ ) [fltarr].	fluxnet
swuptoa	Shortwave upwelling flux at the top of the atmosphere ( $\text{W m}^{-2}$ ) [fltarr].	fluxnet
lwuptoa	Longwave upwelling flux at the top of the atmosphere ( $\text{W m}^{-2}$ ) [fltarr].	

**GLOBAL  
PARAMETER  
VALUES**

MAXPARMS	14	set_globals
MAX_SCREEN_PLOTS	4	set_globals
DISPWIN	0	set_globals
MISSING	9999.	set_globals
TRUE	1	set_globals
FALSE	0	set_globals
CLEAR	0	set_globals
CLOUDY	1	set_globals
BAD	2	set_globals
WATPHASE	0	set_globals
ICEPHASE	1	set_globals
LAND	254	set_globals
NOTLAND	0	set_globals
OCEAN	0	set_globals
ICE	3	set_globals
SNOW	4	set_globals
UNIX	1	set_globals
DOS	2	set_globals
SHL_EXT	The character filename extension for shared C libraries	set_globals
SHL_DIR	The directory of the C shared object libraries.	set_globals
CASPR_DIR	The path to the main <b>caspr</b> directory.	set_globals
DIRCHAR	'/' for Unix and '\' for MSDOS	set_globals
WFONT	Font used for the <b>wcaspr</b> and <b>wplot</b> widgets	set_globals
WDEV	Windowing device (from !d.name)	set_globals
DARKZEN	Solar zenith angle cutoff for "dark" (85)	set_globals
DEBUG	Reserved for future use.	set_globals
NOWARNINGS	Set to the value of the <i>no_warn</i> option in <b>caspr</b> .	set_globals

---

## PROCEDURES

The tables below list the primary procedures and data files in the CASPR system. The hierarchy is illustrated via indentation; e.g., **caspr** calls **ingest\_image** which in turn calls **read\_avhrr**. Utility procedures are not listed here.

Procedure	Functionality	File
caspr	Main procedure.	caspr.pro
read_argfile	Reads <b>caspr</b> argument values from a file.	readarg.pro
set_requests	Translates user parameter requests to internal requests.	requests.pro
read_latlon	Reads the latitude/longitude grids.	reading.pro
read_landmask	Read the land mask.	reading.pro
prof_latlon	Computes a grid of lat/lon corresponding to the temp/humidity profile grid.	profgrid.pro
ingest_image	Reads one image and computes channel combinations.	reading.pro
read_avhrr	Reads an image.	reading.pro
readusr_avhrr	Reads user-defined AVHRR.	usrimg.pro
check_avhrr	Does a rough check for bad data.	reading.pro
normalize	Normalizes channels 1, 2, and 3A by the solar zenith angle.	convert.pro
esdist_correct	Corrects channels 1 and 2 albedo for Earth-Sun distance variations.	convert.pro
change_input_units	Changes input image units from integer to float, etc.	convert.pro
ch3reflectance	Computes the channel 3 reflectance.	convert.pro
cloudmask_n	Performs the time series cloud masking.	cldmaskn.pro
cloudmask_1	Performs the single-image cloud masking.	cldmask1.pro
cloudfrac	Computes the cloud fraction for subregions.	cldprops.pro
profgrid	Sets up the temperature and humidity profiles.	profgrid.pro
getusrprof	User-defined profiles.	usrprof.pro
o3aer	Climatological ozone and aerosol optical depth.	profgrid.pro
geto3	Reads/assigns an ozone grid for a particular time	profgrid.pro
getaer	Reads/assigns an aerosol optical depth value for a particular time	profgrid.pro
retrieve	Calls all the retrieval procedures.	retrieve.pro
surftypes	Relabels the input land mask for additional surface types.	surftype.pro
precip_water_prof	Precipitable water from profiles.	prewater.pro,c
surftemp_clear	Clear sky surface temperature.	surftemp.pro,c
precip_water_avhrr	Clear sky precipitable water from AVHRR.	prewater.pro,c
narr2bb_toa	Narrow to broadband conversion at TOA.	acorrect.pro,c
anis_correct	Anisotropic reflectance correction of TOA albedo.	acorrect.pro,c
atmos_correct	Atmospheric correction of TOA albedo.	acorrect.pro,c
clearcomposites	Performs the clear sky compositing	clrcomp.pro
fill_clear	Fills in clear values for certain arrays.	fillclr.pro
cloudphase	Cloud particle phase.	cldphase.pro
cloudretau	Performs the cloud optical depth and particle effective radius retrievals.	cldretau.pro, cldretau.c
cloudtemp	Cloud top temperature.	cldtemp.pro
cloudpress	Cloud top pressure.	cldtemp.pro
cloudwc	Cloud water content (constants)	cldtemp.pro
surfalb_cloudy	Cloudy sky broadband surface albedo.	surfalb.pro
surftemp_cloudy	Cloudy sky surface temperature.	surftemp.pro
fluxnet	Computes the surface radiative fluxes with <i>FluxNet</i> .	fluxnet.pro,c
display_results	Displays the results on the screen.	display.pro
setup_display	Sets up the screen display for results.	display.pro
plot_profile	Plots the temperature and humidity profile.	display.pro
plot_image	Makes an image of the parameter, mapped or not mapped	display.pro
plot_series	Makes a time series plot.	display.pro
plot_hist	Makes a histogram plot.	display.pro

write_results	Writes the results arrays and means to files.	results.pro
wcaspr	The CASPR widget interface.	wcaspr.pro
wplot	Widget-based plotting.	wplot.pro
read_results_image	Reads the parameter results file for an image.	results.pro
read_results_means	Reads the parameter mean results.	results.pro
read_cmask	Reads the full resolution cloud mask.	results.pro
average_area_results	Computes averages over an area.	average.pro
average_time	Computes averages over time.	average.pro
area_results	Determines the mean parameter values around a point.	validate.pro
nfiles_area_results	Determines the mean parameter values around a point in multiple files.	validate.pro
validate	Compare CASPR results to <i>in situ</i> observations.	validate.pro
read_insitu	Reads in situ observations for input to <b>validate</b> .	usrobs.pro
write_subset	Reads and subsets and/or subsamples image files if only a small region needs to be examined.	subset.pro
write_subset_results	Reads and subsets and/or subsamples <u>results</u> image files if only a small region needs to be examined.	subset.pro
write_netcdf_*	Write the parameters, cloudmask, lat-lon arrays, etc. in netCDF format	netcdf.pro
read_netcdf_*	Read the parameters, cloudmask, lat-lon arrays, etc. that were written in netCDF format by 'write_netcdf_*'.	netcdf.pro

## USER-MODIFIABLE PROCEDURES

As listed above, there are a few procedures that must be modified by the user under certain circumstances. If you wish to supply the satellite data in a format other than what CASPR expects then you should modify the procedure **readusr\_avhrr** in the file **usrimg.pro**. To supply your own temperature and humidity profiles you must modify **getusrprof** in the file **usrprof.pro**. You may also want to change the default ozone and aerosol optical depth data. The procedures to change are **geto3** and **getaer**, also in **usrprof.pro**. Lastly, if you are performing validation you'll need to read your in situ observations with the procedure **read\_insitu** in the file **usrobs.pro**. With all of these you should follow the instructions in the procedure headers.

## BATCH FILES

Batch File	Description
cmake.pro	Compiles the CASPR procedures, sets up common blocks and defines some global variables, changes the IDL prompt.
cexit.pro	Restores the IDL prompt and undefines the CASPR global variables (frees memory).
run.pro	A sample call to the main routine <b>caspr</b> . In the <b>test</b> subdirectory.



---

# PART II: REFERENCE

---

Part II of the *CASPR User's Guide* describes data preprocessing and the methods used in the retrieval of surface temperature, surface albedo, atmospheric water vapor, cloud amount, optical depth, particle effective radius, phase, temperature, and pressure, and the surface radiative fluxes. For those algorithms that are published, only minimal algorithm descriptions are given here.

# 1. PROCESSING OVERVIEW

---

The overall processing scheme involves six groups of calculations: the cloud mask, clear sky surface parameters, clear sky surface images, cloud parameters, cloudy-sky surface parameters, and radiative fluxes. This order is dictated by the fact that cloud and surface properties are input to the radiative fluxes, and some surface and clear sky properties are required for the cloud retrievals.

If the input land mask only contains LAND and NOTLAND categories, the surface types are refined by using clear sky reflectances and brightness temperatures. LAND and NOTLAND are subdivided into snow-covered and snow-free land, open water, and ice. The clear sky surface temperature and albedo are then computed. Precipitable water is computed from the satellite data if atmospheric temperature and humidity profiles are not present.

Clear sky images for the surface temperature, precipitable water, and channels 2 and 4 values are created by interpolating the clear values to cloudy pixels. These are needed in subsequent calculations of cloud properties, cloudy sky surface temperature and albedo, and radiative fluxes. This is a very important, and usually error prone, step. In situations where cloud cover is extensive, values that are used to fill cloudy pixels may have come from a great distance, and therefore may be significantly different from the true value. Additionally, false identifications of clear pixels (i.e., cloud contamination) can create significant errors.

The cloud particle phase, effective radius, optical depth, temperature, and pressure are computed next. Cloudy sky surface temperature and albedo, then radiative fluxes complete the calculations.

The following sections describe these steps in detail.

## 2. CONVERSION OF AVHRR CHANNEL INFORMATION

---

CASPR assumes that all AVHRR channels are calibrated. Standard calibration can be done according to the procedures and data given in the NOAA Polar Orbiter Data User's Guide (NOAA, 1991) and the NOAA KLM User's Guide (<http://www2.ncdc.noaa.gov/docs/klm>). The thermal channel calibration should include the non-linear correction (NOAA, 1991). Channels 1 and 2 should have time-dependent calibrations for NOAAs 7, 9, 11, and 14, and the standard calibration for other satellites. As part of the NOAA/NASA AVHRR Pathfinder Calibration Working Group activities, the in-orbit degradation of channels 1 (0.6  $\mu\text{m}$ ) and 2 (0.9  $\mu\text{m}$ ), which are not calibrated on-board, has been determined using the southeastern Libyan desert as a time-invariant calibration target. A statistical analysis of the data over the calibration target show that channels 1 and 2 of NOAA 9 had degraded at the rate of 5.9% and 3.5% per year respectively. The relative variations of the gain were anchored to "absolute" calibrations based on concurrent aircraft and satellite measurements made over the White Sands area of New Mexico. Rao (1993) presents simple formulae and a look-up table for the time-dependent calibration of these two channels for NOAA 9; calibration coefficients for other NOAAs 7 and 11 can be obtained from NOAA/NESDIS (M. Jones, pers. comm., 1994), and the method and data for NOAA 14 can be found at <http://orbitnet.nesdis.noaa.gov/ora/text/nrao02.txt>.

The usual calibration methods for channels 1 and 2 do not include a correction for variations in the Earth-Sun distance over the course of the year. Such a correction is optional here, and is done as follows:

$$\alpha' = \alpha \left( \frac{R_{jday}}{R_{mean}} \right)^2 \quad (1)$$

where  $\alpha'$  is the corrected albedo,  $\alpha$  is the albedo computed using the mean Earth-Sun distance,  $R_{jday}$  is the actual Earth-Sun distance for the day of the year  $jday$ , and  $R_{mean}$  is the mean distance.

Three other spectral "images" are required for the retrieval of surface and cloud properties: the reflected portion of channel 3, the differences between channels 3 (3.7  $\mu\text{m}$ ) and 4 (11  $\mu\text{m}$ ) at night, and the difference between channels 4 and 5 (12  $\mu\text{m}$ ). At 3.7  $\mu\text{m}$ , AVHRR channel 3 contains both reflected solar and emitted thermal components. The reflected portion is **approximated** by removing from the total radiance an estimate of the emitted portion, based on the temperature of channel 4 (e.g., Allen et al., 1990):

$$\rho_3 = \frac{L_3 - B_3(T_4)}{L_0\mu - B_3(T_4)} \quad (2)$$

where  $\rho_3$  is the channel 3 reflectance,  $L_3$  is the channel 3 radiance,  $B_3(T_4)$  is the Planck function for channel 3 based on the channel 4 temperature  $T_4$ ,  $L_0$  is the solar constant for the band (adjusted for Earth-Sun distance), and  $\mu$  is the cosine of the solar zenith angle. Equation 2 is derived from the basic relationship

$$L_3 = \epsilon_3 B_3(T_4) + \rho_3 L_0 \mu$$

where  $\epsilon_3 = 1 - \rho_3$  is the emissivity. This relationship assumes that the surface or cloud in the field-of-view do not transmit any radiation, and that emission and reflection are isotropic. Without any a priori knowledge of the scene, these assumptions are necessary. The difference between channels 4 and 5 and between channels 3 and 4 at night are a simple arithmetic subtraction of brightness temperatures.

### 3. SURFACE PROPERTIES

---

#### SURFACE TEMPERATURE

For the retrieval of clear sky surface temperature a simple regression model is used to correct for atmospheric attenuation. For high-latitude ocean and snow-covered land we use the equation

$$T_s = a + bT_4 + c(T_4 - T_5) + d[(T_4 - T_5)(\sec\theta - 1)] \quad (3)$$

where  $T_s$  is the surface temperature,  $T_4$  and  $T_5$  are the satellite measured brightness temperatures in channels 4 and 5,  $\theta$  is the sensor scan angle, and  $a$ ,  $b$ ,  $c$ , and  $d$  are regression coefficients. To determine the empirical relationship in (3), radiosonde data from drifting ice and land stations in the Arctic and Antarctic were used with a radiative transfer model to simulate the sensor brightness temperatures.

The regression method of relating modeled brightness temperatures to surface temperature was also used for a snow-free land algorithm. But because spectral emissivities for vegetation in channels 4 and 5 are variable and generally unknown, they are variables in the regression. Additionally, scan angle is not a variable in the regression since its dependence on angular emissivity is unknown. The regression equation for snow-free land has the form:

$$T_s = a + bT_4 + cT_5 + d\varepsilon_4 + e\varepsilon_5 \quad (4)$$

where  $\varepsilon_i$  is the emissivity in channel  $i$ . The surface temperature retrieval methods for both sea ice/snow and snow-free land are described in detail in Key, et al. (1997).

The cloudy sky surface temperature calculation is based on empirical (linear regression) relationships between the clear sky temperature, wind speed, and solar zenith angle (daytime), determined using surface observations from the SHEBA (Surface HEat Budget of the Arctic) experiment. **It applies only to sea ice.** The clear sky surface temperatures are interpolated to cloudy pixels with a kriging function, then the cloudy sky temperatures are estimated from these clear temperatures and one or two other variables, depending on the time of year. For the polar night and before the melt season (November through April) there are two equations:

- solar zenith angle 80 degrees or more:  $T_{cld} = a_1 + b_1 * T_{clr} + c_1 * u_{cld}$   
solar zenith angle less than 80 degrees:  $T_{cld} = a_2 + b_2 * T_{clr} + c_2 * \cos(Z) + d_2 * u_{cld}$

During the warm season, defined as May-September with the surface temperature greater than 255K, the following apply:

- solar zenith angle less than 90 degrees:  $T_{cld} = a_3 + b_3 * T_{clr} + c_3 * \cos(Z) + d_3 * t_{cld}$   
or:  $T_{cld} = a_3 + b_3 * T_{clr} + c_3 * \cos(Z)$
- nighttime only:  $T_{cld} = a_4 + b_4 * T_{clr} + c_4 * u_{cld}$

where  $T_{cld}$  is the cloudy sky surface temperature (K),  $T_{clr}$  is the clear sky surface temperature (K),  $u_{cld}$  is



the cloudy sky wind speed ( $\text{m s}^{-1}$ ),  $Z$  is the solar zenith angle,  $t_{cld}$  is the number of hours that it has been cloudy. Because  $t_{cld}$  will not generally be known to better than six hours with satellite data, the alternate equation is used in CASPR. This procedure is unpublished.



### CAUTION

If you don't have wind speed data, comment out the call to `surftemp_cloudy` in `retrieve.pro`. Using a wind speed of 0 is not a valid workaround! At present this procedure should be considered experimental.



### CAUTION

The largest potential source of error in the cloudy sky surface temperature is the interpolation of clear sky values to cloudy areas. This is particularly true for single image processing (as opposed to the time series approach). Cloudy sky results in coastal areas and areas of extensive cloud cover have large uncertainties!

## SURFACE ALBEDO

The retrieval of surface albedo involves four steps:

1. Convert channels 1 and 2 narrowband reflectances to a broadband reflectance.
2. Correct the top-of-atmosphere (TOA) broadband reflectance for anisotropy.
3. Convert the TOA broadband albedo to a surface broadband albedo.
4. Adjust the surface clear sky broadband albedo for the effects of cloud cover in cloudy pixels (snow/ice only).

The general methodology described by steps 1-3 was used by Csiszar and Gutman (1999) for global land studies. In CASPR, relationships for land and ocean were developed independent of that study, and methods for snow/ice and ocean were added. DeAbreu et al. (1994), Lindsay and Rothrock (1994), and earlier versions of CASPR used a procedure where the anisotropic reflectance correction was applied to channels 1 and 2, an atmospheric correction was done on those channels, then narrowband albedos were converted to broadband. In CASPR that procedure tended to overestimate the albedo of snow/ice.

It is important to distinguish between "inherent" and "apparent" surface albedos. The inherent albedo is the "true", no-atmosphere, or "black-sky" albedo of the surface and is independent of changes in atmospheric conditions. The apparent albedo is what would be measured by up- and down-looking radiometers in the field. It varies with atmospheric conditions. Both vary with solar zenith angle and are directional in that regard. The difference between them is very small for the ocean but can be large for vegetation and snow. Figure 1 gives an example of the difference between these two albedo types for ocean, vegetation, and snow. As the figure illustrates, differences can be up to 10%. **CASPR calculates the directional-hemispherical apparent albedo**, although it also contains code to calculate the inherent albedo. After the apparent albedo is calculated it is adjusted for cloud cover. The complete procedure is detailed in Key et al. (2001).

The first step is to convert the narrowband reflectances in AVHRR channels 1 and 2 to a TOA

broadband reflectance. This is necessary because the anisotropic reflectance correction in step 2 requires a broadband reflectance. The narrow-to-broadband conversion takes the form

$$\rho_{toa} = a + b\rho_{1,toa} + c\rho_{2,toa} \quad (5)$$

where  $\rho_{1,toa}$  is the channel 1 reflectance,  $\rho_{2,toa}$  is the channel 2 reflectance,  $\rho_{toa}$  is the broadband TOA reflectance, and  $a$ ,  $b$ , and  $c$  are regression coefficients. To develop the regression relationship *Streamer* was used to simulate the TOA reflectances over a broad range of viewing and illumination angles, atmospheric conditions (aerosol optical depth and water vapor amount), and surface types and albedos. Separate sets of coefficients were determined for snow/ice and snow-free land (generic vegetation in *Streamer*). For open ocean the broadband reflectance is set to the channel 1 reflectance.

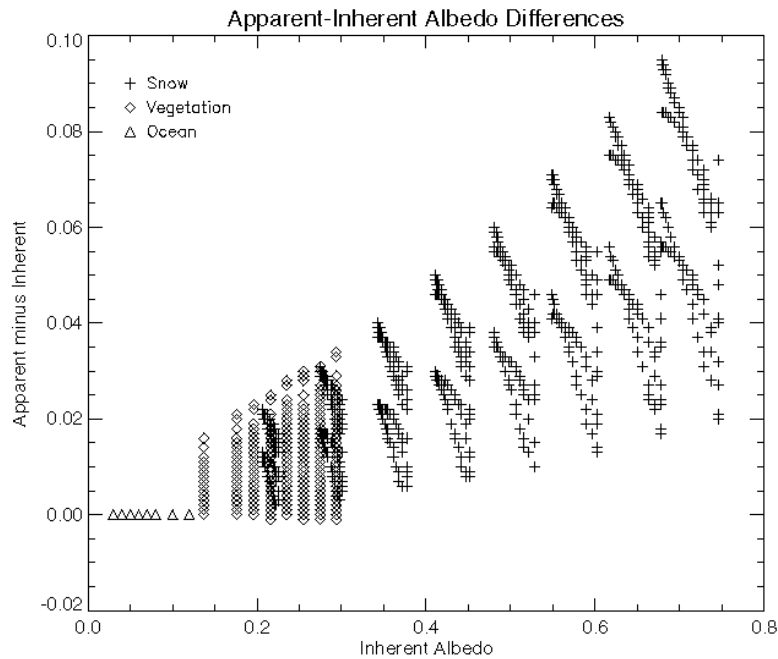


*Figure 1.* The difference between the apparent (atmosphere dependent) and inherent surface albedos of unfrozen ocean, snow-free land (vegetation), and snow. Data are from radiative transfer model calculations (*Streamer*) for two precipitable water amounts (0.5 and 5 g cm<sup>-2</sup>), two aerosol optical depths (0.05 and 0.5), and solar zenith angles from 0 to 87 degrees.

The next step is to correct for the dependence of the sun-satellite-surface geometry on reflectance. This is done with data presented in Suttles et al. (1988). That study used ERBE and GOES data to determine TOA anisotropic reflectance factors (ARF) for the broad shortwave band over various surfaces. It updates the earlier work of Taylor and Stowe (1984). Both the ERBE and GOES instruments measure radiances and are therefore a function of viewing and illumination geometry. To convert the directional reflectance to albedo, the ERBE/GOES ARFs are used:

$$\alpha_{toa} = \frac{\rho_{toa}}{f} \quad (6)$$

where  $\rho_{toa}$  is the reflectance observed at the sensor (simulated by *Streamer* in step 1),  $f$  is the anisotropic reflectance factor, and  $\alpha_{toa}$  is the TOA albedo, which is only a function of solar zenith angle. A trilinear interpolation routine was used to retrieve  $f$  as a function of satellite zenith angle, solar zenith angle, and the relative azimuth angle.

Next, the broadband, clear sky, apparent surface albedo is estimated with a regression relationship of the form

$$\alpha_{toa} = a + b\alpha_s \quad (7)$$

where  $\alpha_s$  is the surface reflectance, and  $a$  and  $b$  are a function of water vapor, aerosol amount, and solar zenith angle. There is a different set of coefficients for each solar zenith angle, aerosol optical depth, and precipitable water bin. This method was used by Koepke (1989) for AVHRR channels 1 and 2 separately. Here the coefficients were determined with *Streamer* for a variety of surface and atmospheric conditions and illumination angles. Viewing geometry is not important in this step. Snow/ice and vegetation surface types were used in the radiative transfer calculations, and the regression coefficients are based on the combined surface type data. For ocean surface albedo a simpler approach is used:

$$\alpha_s = a + b\alpha_{toa} + c\cos Z + dPW + e\tau_{aer} \quad (8)$$

where  $PW$  is precipitable water (cm),  $\tau_{aer}$  is aerosol visible optical depth (unitless),  $Z$  is the solar zenith angle, and  $a$ ,  $b$ ,  $c$ ,  $d$ , and  $e$  are regression coefficient based on modeled albedos.

The surface albedo under clear and cloudy conditions can be very different. This is illustrated in Figure 2 which shows the change in surface albedo with increasing optical depth. The values are fractional change, where 1 means no difference between clear and cloudy values. While the cloudy sky albedo can be 15% more or less than the clear sky value for both surface types, it is consistently higher for snow, with a mean difference near 10%. For vegetation, the cloudy albedo may be higher or lower, so that the mean difference is very small. For this reason, only the snow albedo is adjusted for cloud cover.

The albedo of cloudy pixels is determined using the clear sky albedo, interpolated to fill in the entire image, adjusted by the cloud optical depth and the solar zenith angle. This conversion is also based on model calculations, where *Streamer* was used to compute upwelling and downwelling fluxes for a snow/ice surface over a range of cloud and atmospheric conditions. The empirical relationship between the clear sky broadband albedo, cloud optical depth, and the cloudy sky broadband surface albedo is

$$\alpha_{s, cld} = a + b\alpha_{s, clr} + c\ln(\tau + 1) + d\cos Z \quad (9)$$

where  $\tau$  is the cloud visible optical depth (unitless),  $\alpha_{s, clr}$  is the clear sky **apparent** albedo (see above),  $Z$  is the solar zenith angle, and  $a$ ,  $b$ , and  $c$  are regression coefficients. As aerosol and water vapor amounts are not explicit in this relationship, this adjustment assumes that their effect on the surface albedo is small relative to that of clouds. Note, however, that this adjustment is to the apparent albedo, which is a function of aerosol and water vapor amounts. No distinction is made between water and ice clouds, although both were included in the model data for the regression analysis. This relationship works best when the snow surface is bright ( $\alpha > 0.5$ ) and clouds have small to moderately large optical depths ( $1 < \tau < 50$ ). For snow-free land and open water the cloudy sky broadband albedo is set to the clear sky broadband value.

In the model calculations of steps 1, 3, and 4, the variable ranges were as follows: solar zenith angle: 0 - 87 degrees, aerosol visible optical depth: 0.05 - 0.5, precipitable water: 0.5 - 5 g m<sup>-3</sup>, snow visible albedo: 0.5 - 0.99, and vegetation visible albedo: 0.07 - 0.15. In all cases ozone amount was prescribed at

325 Dobson units.

Note: No albedo retrievals are done for solar zenith angles greater than the variable DARKZEN, which is currently set to 85 degrees. Figure 3 shows the latitudes and times of the year where solar zenith angles greater than 85 degrees are experienced. Surface albedo retrievals will not be done for latitudes above the dashed line on a particular day.



### **CAUTION**

The largest potential source of error in the cloudy sky surface albedo is the interpolation of clear sky values to cloudy areas. This is particularly true for single image processing (as opposed to the time series approach). Cloudy sky results in coastal areas and areas of extensive cloud cover have large uncertainties!

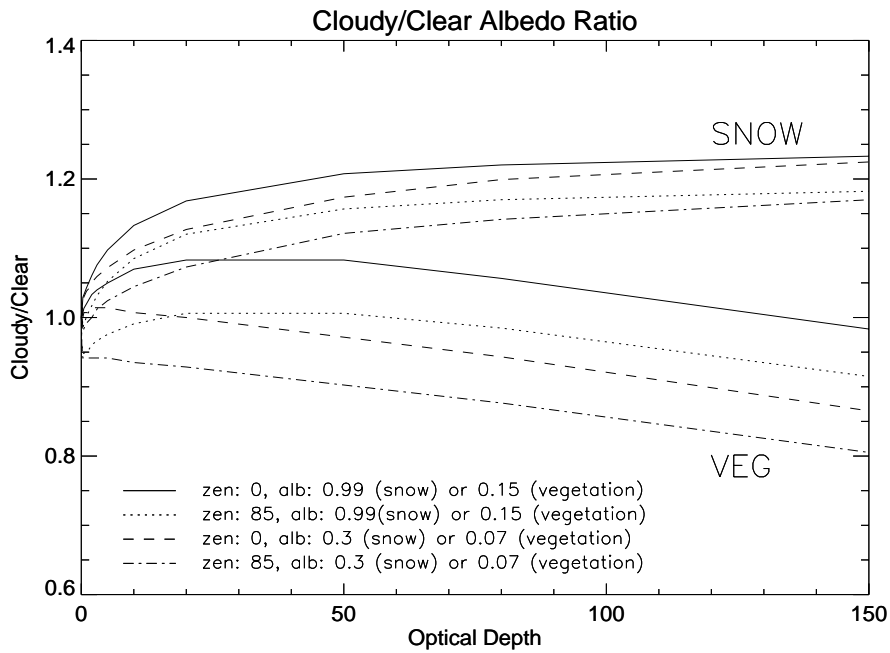


*Figure 2.* Differences between clear and cloudy surface albedos expressed as a fraction (cloudy divided by clear; 1 means no difference) for snow (top set of lines) and generic vegetation (bottom set), given as a function of cloud optical depth. Results were generated with a radiative transfer model for water and ice cloud under varying atmospheric conditions. The lines are for different solar zenith angles (0 and 85 degrees) and visible surface albedos (0.3 and 0.99 for snow; 0.07 and 0.15 for vegetation).

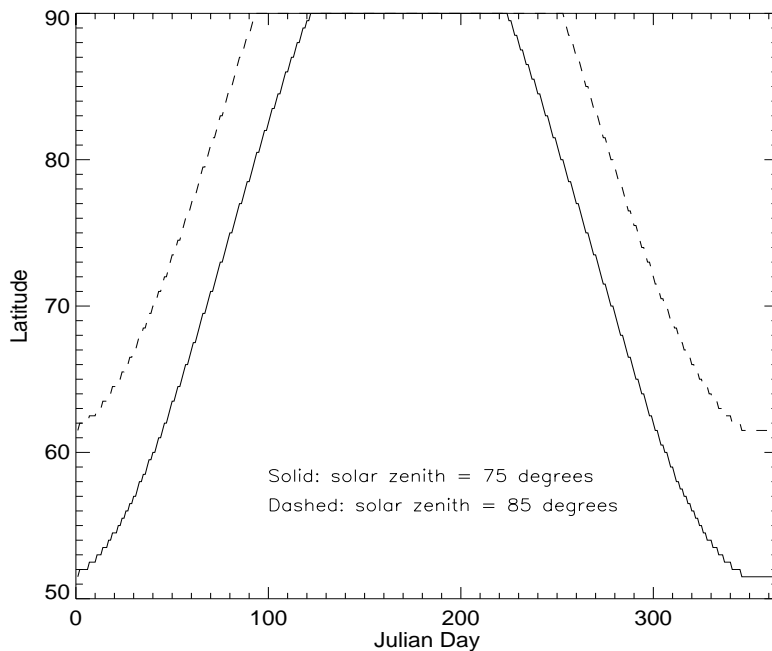


*Figure 3.* Latitudes and times of the year where zenith angles greater than 85 degrees and greater than 75 degrees are experienced at solar noon. All latitudes poleward of those shown will have solar zenith angles larger than 85 or 75 degrees. The 85 degree line is relevant to albedo retrievals; the 75 degree line is relevant to cloud optical depth retrievals.

## 4. WATER VAPOR

---

The total precipitable water in the atmospheric vertical column is needed for the surface albedo, cloud optical depth, and radiative flux calculations. It may be computed from the humidity profile, if available, or estimated from the satellite data using the split-window thermal channels. The preferred method is to compute it from the humidity profile, and that will be done if it is available. **This split-window technique has a large uncertainty**, as neither of the channels are very sensitive to water vapor (which is why they are window channels!).

The procedure is to convert relative humidity to mixing ratio, then integrate mixing ratio over all layers, using the mean of two adjacent levels as the representative value of the layer:

$$PW = 100 \sum_{i=1}^{n-1} \frac{w}{g\rho} (p_i - p_{i+1}) \quad (10)$$

where  $PW$  is precipitable water (cm),  $w$  is the mixing ratio (g/g),  $g$  is gravitational acceleration ( $9.8 \text{ m s}^{-2}$ ),  $\rho$  is the density of water ( $1000 \text{ kg m}^{-3}$ ),  $p$  is pressure (Pa), and  $n$  is the number of vertical levels with  $i=1$  being the surface.

If the humidity profile is not available, the precipitable water will be estimated for clear sky areas using the AVHRR thermal channels. At high latitudes the relationship is:

$$PW = \exp[-10.4974 + 0.751008(T_4 - T_5) + 0.0453005T_5] \cos \theta \quad (11)$$

where  $PW$  is precipitable water (cm),  $T_4$  and  $T_5$  are the satellite measured brightness temperatures in channels 4 and 5, and  $\theta$  is the sensor scan angle. The coefficients were determined over a range of surface temperatures and water vapor amounts typical of the Arctic using modeled AVHRR radiances as in the surface temperature algorithm. This procedure is for clear-sky pixels only. It is far less reliable (and more variable) than using a humidity profile.

## 5. CLEAR SKY COMPOSITES

---

A critical step in time series cloud detection, and an optional step in single image processing, is clear sky compositing. This involves creating a clear sky image for various channels or parameters, which means filling in cloudy areas with clear values. This is a very important, and usually error prone, step. In situations where cloud cover is extensive, values that are used to fill cloudy pixels may have come from a great distance in space or time, and therefore may be significantly different from the true value.



### CAUTION

The largest potential source of error in the cloudy sky surface temperature and albedo is the interpolation of clear sky values to cloudy areas. This is particularly true for single image processing (as opposed to the time series approach). Cloudy sky results in coastal areas and areas of extensive cloud cover have large uncertainties!

This step is necessary for two reasons: (1) In time series cloud detection the clear sky images are used in a final thresholding operation, where the actual radiance data are compared to the estimated clear sky values and a new cloud/not-cloud determination is made. (2) The retrieval of some cloud properties, and the calculation of surface radiative fluxes, require values for the surface under the cloud.

In time series cloud detection, and optionally with single-image processing (see the keyword *clear\_composite*), clear sky statistics are compiled for each pixel using all clear values within some distance of the pixel and over some number of days (typically 150x150 km cells and 5 days). Medians of the required channels and parameter data are computed. If a cell occurs along a coastline, only pixels with the same surface type (LAND or NOTLAND) as the center pixel are used. Pixels in the clear sky composite that did not have medians assigned due to the lack of clear values are filled by a kriging interpolation procedure. The probability of finding clear pixels can be increased by enlarging the cell size or using more days, but doing so also increases the variability and may adversely affect the next step.

The compositing procedure therefore involves two steps: computing median values for each pixel over a small region in space and time, and filling in those pixels that did not receive a clear sky estimate with an interpolation procedure. In time series cloud masking both are an integral part of the procedure; they are not optional. But after the cloud detection step, whether in time series mode or not, clear sky compositing can be done (again, see the *clear\_composite* keyword). The filling/interpolation will be done whether or not clear compositing is done, the only difference being that in one case the clear images are based on clear values from the current image only; in the other case it is based on clear values from the current and previous images.

If clear sky compositing is done, the maximum clear sky channel 4 temperature is written to a separate file. This can be used to improve single image cloud detection via the *tsurfest* keyword to *caspr*. See the section on *File Input and Output* in the *User's Guide* for more information.

## 6. CLOUD PROPERTIES

---

### RADIATIVE TRANSFER MODEL

Cloud detection and the retrieval of cloud optical depth and particle effective radius rely heavily on modeled TOA albedo and brightness temperature. Before detailing those procedures, the radiative transfer model *Streamer* (Key and Schweiger, 1998) is briefly described. TOA radiances (intensities) are computed for use in the cloud property retrievals while irradiances (fluxes) are computed in order to examine the surface radiation budget. For radiances *Streamer* uses the discrete ordinate solver DISORT described in Stamnes et al. (1988). For irradiances the two-stream method following Toon et al. (1989) is employed. In both cases there are 24 shortwave and 105 longwave spectral bands. Gas absorption for water vapor, ozone, CO<sub>2</sub> and oxygen is parameterized using an exponential sum fitting technique (Tsay et al., 1989).

Cloud optical properties are based on parameterization schemes from three different sources. For water clouds, the data are taken from Hu and Stamnes (1993). Effective radii range from 2.5 to 60  $\mu\text{m}$  for shortwave and longwave portions of the spectrum. For ice clouds in the shortwave the parameterization of Fu and Liou (1993) is used. Longwave ice cloud optical properties are based on Mie calculations using spherical particles. This parameterization is unpublished but follows the methodology of Hu and Stamnes. Both the water and ice cloud parameterizations are based on the empirical relationship between the particle effective radius and extinction, single scatter albedo, and the asymmetry parameter.

### CLOUD DETECTION

Methods of detecting clouds in satellite data range from simple thresholding procedures to complex neural networks. No attempt is made here to survey the tremendous breadth of this field; instead, a few examples from the literature are given. Ebert (1987) described one of the first polar-specific cloud retrieval algorithms, one that utilized a variety of spectral and textural measures. Key and Barry (1989) implemented a high-latitude method similar to that used in the global algorithm of the ISCCP (Rossow and Garder, 1993) based on spectral, spatial, and temporal variations of clouds. A number of studies have exploited the high reflectivity of liquid water clouds at 3.7  $\mu\text{m}$  during the day (e.g., Allen et al, 1990; Welch et al., 1992; Sakellariou et al., 1993), while only a few have been developed specifically for nighttime retrievals (e.g., Yamanouchi et al., 1987). Most of the cloud detection algorithms are based on empirical relationships derived from a small sample of satellite data.

The cloud masking procedure presented here consists of thresholding operations that are based on modeled sensor radiances. The AVHRR radiances are simulated for a wide variety of surface and atmospheric conditions, and values that approximately divide clear from cloudy scenes are determined. Examples are given in Figures 4 and 5 where the channel 3 reflectance and the thermal channel differences, respectively, are shown as a function of cloud optical depth. Clear sky is represented as having a cloud optical depth of zero.

#### *Single-Image Masking*

The underlying philosophy of the single-image cloud detection procedure is that it should work as well as possible without requiring ancillary information. The target user is one who has a few individual images that are not necessarily part of a time series, and no additional information such as model fields of surface temperature or an elevation database. The single-image cloud mask procedure could be certainly be improved with such information, but it would be unreasonable to require it.

The single image cloud mask uses four primary spectral tests and an optional secondary test. Many of



the cloud test concepts can be found in the Air Force SERCAA procedures (Gustafson et al., 1994); some appear in the NOAA CLAVR algorithm (Stowe et al., 1991); most were developed and/or used elsewhere but refined and extended for use in the polar regions. The application of the spectral tests is conceptually simple: initialize the cloud mask to clear, then apply the spectral cloud tests to label cloudy pixels. The primary spectral cloud tests are described in the following paragraphs. Only two of the four tests are applied under all solar zenith angle (SZA) conditions. One is used only when it is dark; the other is used only when it relatively bright. See Table 1 for SZA cutoffs.

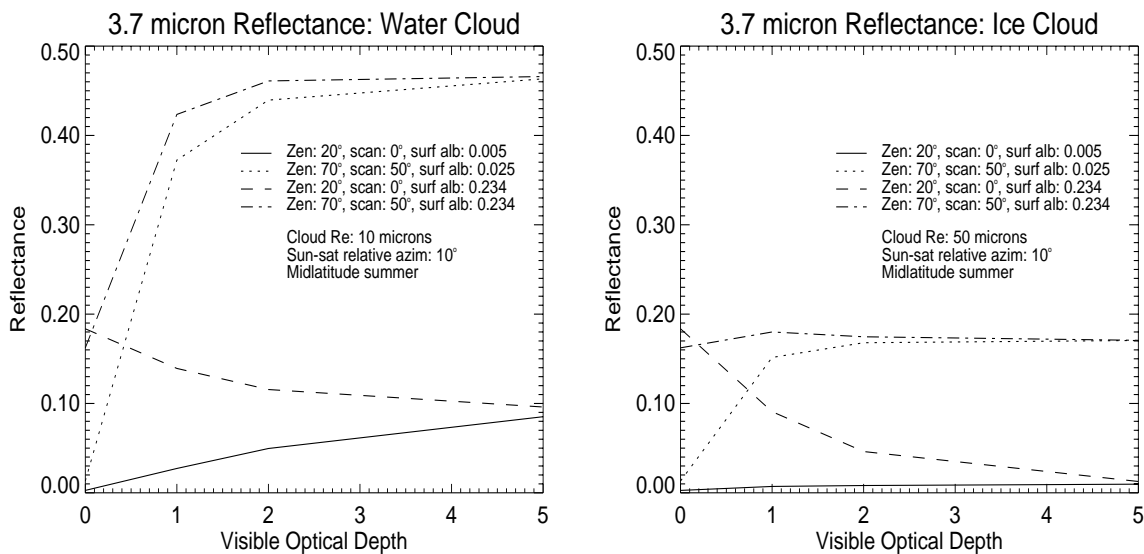


Figure 4. Channel 3 reflectance as a function of liquid (often simply "water") cloud optical depth for a variety of surface and viewing conditions.

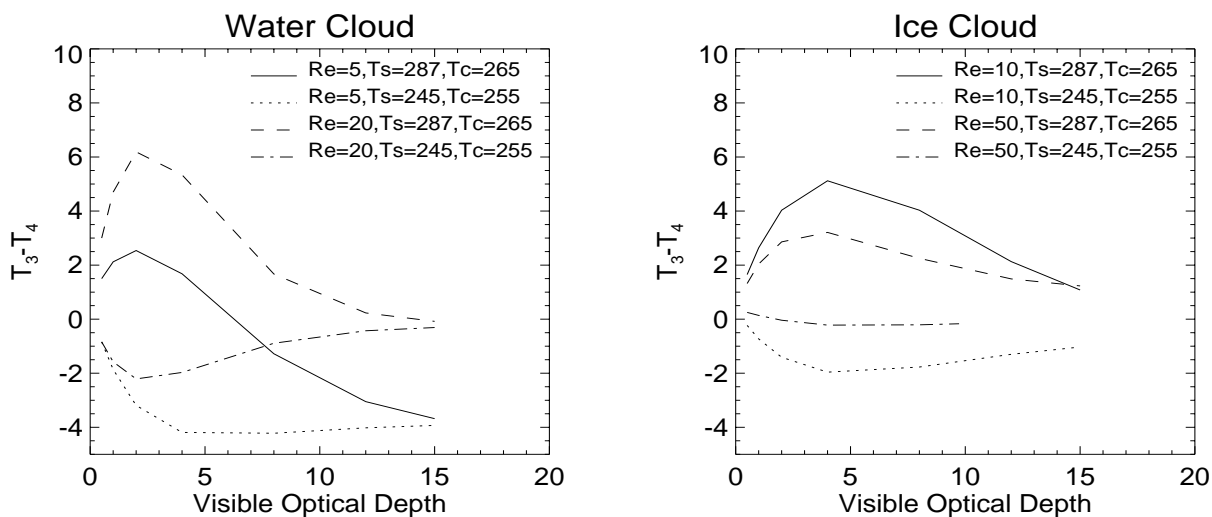


Figure 5. The brightness temperature difference (BTD) of AVHRR channels 3-4 as a function of cloud optical depth for water cloud (left) and ice cloud (right).  $T_c$  is the cloud top temperature,  $Re$  is the cloud particle effective radius.

## Cloud Tests

**Split-Window Cirrus test, 11-12  $\mu\text{m}$  (all SZA)** - Ice clouds absorb and scatter less at 11  $\mu\text{m}$  than at 12  $\mu\text{m}$ , so their transmittances are higher at 11  $\mu\text{m}$ . Water clouds also absorb less at 11  $\mu\text{m}$  but they scatter more. Nevertheless, both ice and liquid clouds have higher transmittances at 11  $\mu\text{m}$ . For cold cirrus clouds and thin water clouds the result is higher brightness temperatures at 11  $\mu\text{m}$ . However, water vapor affects this difference and must be considered. This is accomplished indirectly through the use of the scan angle and brightness temperature. The BT45 differences are corrected for viewing angle effects before being used in any of the cloud tests. Individual pixels are labeled as cloudy if the corrected btd45 is greater than the CT\_THRESH thresholds (Table 2).

CT\_THRESH values are from Saunders and Kriebel (1988) for temperatures of 260 K and greater, with minor adjustments at the low end of the temperature range. For lower temperatures the table was extended by simulating clear sky values with *Streamer* and adding a small offset to account for unmodelled effects. The nadir thresholds are shown in Figure 6. A function that adjusts for the scan angle dependence of BT45 was then determined empirically, with the same functional form as that given by Yamanouchi et al. (1987):

$$BTD45' = BTD45 - \frac{(23.6 - ZC)(1 - \cos\theta)}{1 - 0.1589(1 - \cos\theta)} \quad (12)$$

where ZC is given in Table 2, BTD45 is the unadjusted brightness temperature difference, and  $\theta$  is the scan angle. This effectively adjusts the raw brightness temperature difference to a nadir view. The angle adjustment functions are shown in Figure 7. Note that the sign of the correction changes at approximately 260 K. If BTD45' is greater than CT\_THRESH then the pixel is cloudy. The model simulations assumed that the surface emissivities were the same at 11 and 12  $\mu\text{m}$ . This is probably not the case for snow, so the thresholds are increased by 0.3 K if the surface is known to be snow. This correction should actually be done to radiances, as the emissivity effect is nonlinear in brightness temperature.

**Warm clouds, 11-12  $\mu\text{m}$  (all SZA)** - The transmittance relationships described in the previous test hold true regardless of the relationship between the cloud and surface temperatures. For warm clouds BTD45 may be negative, so an additional test is required (cf., Yamanouchi et al., 1987). A pixel is considered to be cloudy if  $BTD45' < WT\_THRESH$  (Table 2; Figures 6 and 7). Temperature inversions and warm clouds are ubiquitous during the polar night, but also occur at other times of the year and in other locations outside of the polar regions; e.g., over cold ocean currents.

**Water cloud test, 1.6 and 3.7  $\mu\text{m}$  (SZA < NOREFZEN)** - The single-scattering albedo of small droplets at 1.6 and 3.7  $\mu\text{m}$  (AVHRR channels 3A and 3B) is considerably larger than that of ice crystals, including snow on the surface. Therefore, the 1.6 and 3.7  $\mu\text{m}$  reflectances are very high relative to snow, open water, and vegetation. For sunlit scenes the application of reflectance tests depends on the solar zenith angle. For solar zenith angles less than DAYZEN (Table 1) constant thresholds in channels 1 and 3 are applied. A pixel is considered cloudy if  $REF3 > REF3\_OCEAN$  and  $REF1 > REF1\_OCEAN$  or  $REF3 > REF3\_LAND$  and  $REF1 > REF1\_LAND$ , where REF1 and REF3 are the channels 1 and 3 reflectances. There are actually REF3\_OCEAN and REF3\_LAND variables for the 3.7 and 1.6  $\mu\text{m}$  channels, channels 3B and 3A, respectively: REF3A\_OCEAN, REF3B\_OCEAN, REF3A\_LAND, and REF3B\_LAND. The channel referenced by "3B" is channel 3 through NOAA-15 and channel 3B on NOAA-16 and beyond. The visible reflectance test reduces the mislabelling of clear snow-free land and silty water (near mouths of rivers) pixels which have relatively high reflectances at 3.7 microns.

If the zenith angle is between DAYZEN and NOREFZEN then these thresholds are scaled, increasing as a function of the zenith angle. A function was derived empirically:

$$REF3' = REF3 + \left( a \frac{REF3ADD}{b} \right) \quad (13)$$

where REF3' is the adjusted threshold, REF3 and REF3ADD correspond to ocean or land types (Table 1; REF3\*\_ADD),  $a=(SZA-DAYZEN)^3$ , and  $b=(90-DAYZEN)^3$ . The same adjustment is done for the channel 1 reflectance. A pixel is cloudy if it's reflectance is greater than REF3' or REF1'. No reflectance tests are applied to for zenith angles between NOREFZEN and NIGHTZEN. *Note: This effect is still under investigation.*

**Low stratus-thin cirrus tests, 3.7-11  $\mu\text{m}$  (SZA  $\geq$  NIGHTZEN)** - Both ice and water clouds have lower emissivities at 3.7  $\mu\text{m}$  than at 11 or 12  $\mu\text{m}$ . Additionally, small droplets scatter much more efficiently at 3.7  $\mu\text{m}$  than at 11 or 12  $\mu\text{m}$ . For optically thick water clouds, where transmittance is small, this translates into a lower brightness temperature in channel 3. Stratus clouds often exhibit this effect, as do thin, warm clouds (less frequent). For thin, cold clouds the brightness temperature at 3.7  $\mu\text{m}$  can be greater than that at 11  $\mu\text{m}$  because of transmitted radiation from the warm surface in the shorter wavelength band. This is typical of cirrus clouds. A pixel is cloudy if  $BTD34 \leq LSTTCI\_34LO$  or  $BTD34 \geq LSTTCI\_34HI$ , where BTD34 is the brightness temperature difference between channels 3 and 4. Due to the large amount of noise in channel 3 at low temperatures, this test is only performed for temperatures greater than MINTEMP.

**Cloud Cloud - Surface Temperature Tests, 11  $\mu\text{m}$  or  $T_s$  (all SZA regions)** - These tests are intended to detect very cold clouds by comparing the 11 $\mu\text{m}$  brightness temperature to either a climatological surface temperature or a surface temperature estimate. The cold cloud over oceans test is most useful during the summer months at night. It has little effect in the winter or during the daytime, when reflective tests work well. In some sense it performs in a manner similar to the MODIS CO2 high cloud test. It tends to find the cold, optically thick clouds that the thin cirrus, warm cloud, and low stratus tests miss. It is a simple threshold test that utilizes a monthly climatological estimate of the lowest expected surface temperature over the ocean (frozen or unfrozen). If the 11  $\mu\text{m}$  temperature is less than the climatological minimum surface temperature, the pixel is cloudy.

The other cloud cloud - surface temperature test relies on an estimate of the surface temperature input by the user, and is only performed if an estimate of the surface temperature (or 11  $\mu\text{m}$  brightness temperature, both are treated equally) is provided. It is a simple threshold test such that any pixel with an 11  $\mu\text{m}$  brightness temperature less than 20 K below the surface temperature estimate is considered to be cloudy. This is most useful at night during the winter when some optically thick, cold clouds are misidentified as clear sky.

### ***Clear Tests***

To account for potential problems with the cloud tests, particularly the 11-12  $\mu\text{m}$  BTD, tests that confidently identify clear pixels are used. The clear tests are only applied to those pixels labelled CLOUDY by the cloud tests.

**Low NIR reflectance test (DAY and HISZA regions):** This test is the complement of the reflectance cloud test, where pixels with 1.6 or 3.7  $\mu\text{m}$  reflectances less than  $REF3*0.4$  are considered clear.

**NDSI test (DAY and HISZA regions):** The Normalized Difference Snow Index (NDSI; Hall et al.) is used in conjunction with the NIR reflectance for the AVHRR/3 with the 1.6  $\mu\text{m}$  channel (NOAA-16 and higher). If NDSI is large and the NIR reflectance is small, then the pixel is clear. NDSI is calculated as

$$NDSI = \frac{\rho_1 - \rho_3}{\rho_1 + \rho_3} \quad (14)$$

## Rethresholding

The secondary threshold test is a rethresholding operation using only the channel 4 brightness temperatures. It is not employed by default in CASPR, but is available as an option. Using pixels labeled as clear by the primary tests, an average channel 4 temperature image is constructed with a kriging procedure for small regions (200 km over land; 300 km over ocean). During the day ( $SZA \leq NOREFZEN$ ) the 95th percentile clear sky temperature is used; during dim and dark conditions ( $SZA > NOREFZEN$ ) the median is used. During the day, if the channel 4 temperature is more than DEL4DAY degrees less than the clear temperature then it is cloudy. While this test works well in identifying thin cirrus, it results in some false detections near coastlines, and in areas with large variability in elevation it may actually create more problems than it solves. During dim and dark conditions when temperature inversions and warm clouds are common, the test is two-sided. If the channel 4 temperature is more than DEL4LO degrees less than the clear temperature or if it is DEL4HI degrees greater than the clear temperature then it is cloudy.

At night this rethresholding can be important for two reasons: (1) there is less spectral information available and (2) AVHRR channel 3 tends to be noisy at low temperatures, common during the polar night. Concerning the available spectral information, under most conditions optically thick clouds simply cannot be distinguished from clear sky with the three thermal channels alone. This is illustrated for a few cases in Figure 5. The result is false clear detections, i.e., cloudy pixels labeled as clear. Concerning noise in channel 3, it generally results in predictable errors - false cloud detections - so that those pixels not labeled as cloudy by the primary cloud tests are usually clear. So the primary spectral cloud tests at night are expected to result in some false detections for noisy pixels and for optically thick clouds.



### CAUTION

At night, the cloudier the image, the longer the computation time (unless only spectral tests are being done), and the more uncertain the results.

The thresholds can be adjusted collectively through the *threshadj* keyword to the procedures **caspr** and **cloudmask\_1**. This keyword allows the user to adjust the algorithm to be "cloud-conservative" or "clear-conservative". The cloud/clear-conservative decision is necessary because there will always be partly cloudy pixels, mixed phase clouds, mixed clear pixels, etc. that do not fall neatly into one class or the other. However, this is a somewhat crude in that not all thresholds scale linearly. For best results, change the individual thresholds until the desired results are achieved. The *threshadj* keyword is used in the single-image cloud masking mode when clear parameters are computed. A second, clear-conservative mask is generated to increase the likelihood that those pixels labeled as clear actually are clear.

It is assumed here that we have no a priori knowledge of surface characteristics (e.g., surface temperature from the previous day) and no a priori knowledge of the the location of snow/ice. In fact, the only distinction between surface types is land and ocean. Land may be snow-free or snow-covered. Ocean can be open water or sea ice. Additionally, the nighttime procedure does not incorporate any surface type distinction. This severely limits single-image cloud masking accuracy. Having such information would allow the use of additional spectral cloud tests (e.g., the channel 2/1 ratio over snow-free land), and would allow "tighter" thresholds.

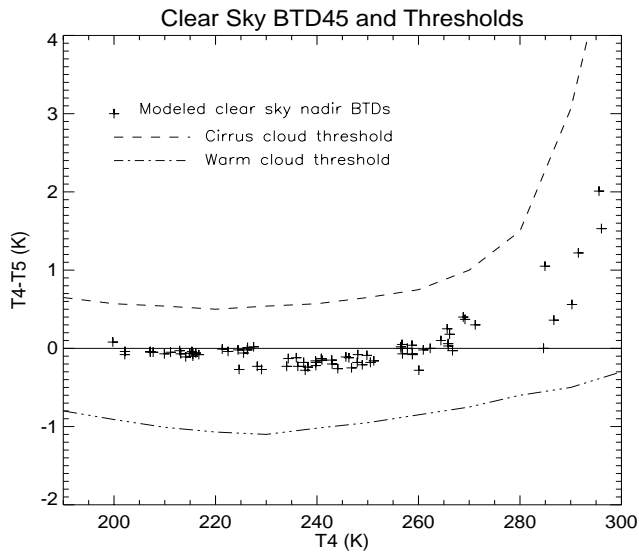


Figure 6. Modeled (*Streamer*) clear sky brightness temperature differences (plus signs) the the cirrus and warm cloud test thresholds (dashed and solid lines, respectively).

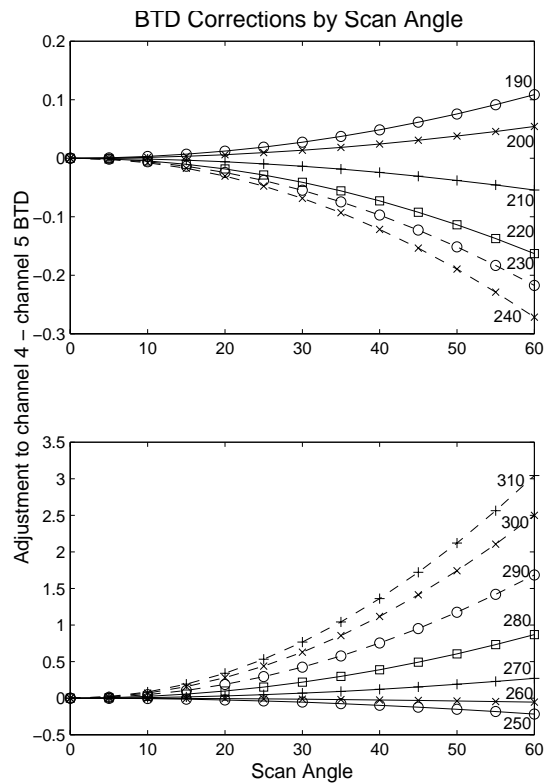


Figure 7. Brightness temperature difference dependence on scan angle. These functions are used to adjust brightness temperature differences before application of the cirrus and warm cloud tests.

*Table 1.* Thresholds used in cloud detection.

Threshold Variable	Value
DAYZEN	60
NOREFZEN	85
NIGHTZEN	88
DEL4DAY	8.0
DEL4LO	4.0
DEL4HI	4.0
REF3A_OCEAN	0.04
REF3B_OCEAN	0.1
REF1_OCEAN	0.35
REF3A_LAND	0.40
REF3B_LAND	0.09
REF1_LAND	0.35
REF3A_OCEAN_ADD	0.0
REF3B_OCEAN_ADD	0.0
REF3A_LAND_ADD	0.15
REF3B_LAND_ADD	0.15
REF3A_SNOW_ADD	0.5
REF3B_SNOW_ADD	0.5
REF1_OCEAN_ADD	0.10
REF1_LAND_ADD	0.15
LSTTCI_34LO	-1.0
LSTTCI_34HI	3.5

Table 2. Brightness temperature difference thresholds for the cirrus cloud test as a function of temperature (K).

	190	200	210	220	230	240	250	260	270	280	290	300	310
CT_THRESH	0.45	0.37	0.34	0.34	0.34	0.40	0.50	0.75	1.00	1.50	3.06	5.77	9.41
WT_THRESH	-0.8	-0.91	-1.01	-1.07	-1.1	-1.02	-0.95	-0.85	-0.75	-0.6	-0.5	-0.3	-0.15
ZC	23.4	23.5	23.7	23.9	24.0	24.1	24.0	23.7	23.2	20.5	19.7	19.0	18.0

### *Time Series Masking*

The time series cloud masking procedure operates on a sequence of images acquired on consecutive days at approximately the same solar time. It first applies spectral tests for an initial labeling of cloudy and clear pixels, then further refines the identification of clear pixels by examining changes in spectral characteristics from one day to the next. The clear pixels that result from these spectral and temporal tests are used to construct a clear sky radiance statistics over some number of days for various spectral channels. The statistics are then used in a final thresholding operation to label/relabel pixels as either clear or cloudy. More specifically the steps are:

1. Apply the single-image cloud mask procedure to identify pixels that are likely to be cloudy. This alleviates the problem of persistent cloud being labelled as clear in the time tests.
2. Examine the time change in spectral characteristics between pairs of days. A pixel is clear if the spectral tests (step #1) say it not cloudy and if it varies little from one day to the next. The channel 4 brightness temperature and the adjusted brightness temperature difference (4-5) are used in the dark parts of the image; these plus the channel 1 reflectance, and the channel 3 reflectance are used in the sunlit portions. Table 3 give the thresholds used in this step (TIME\*).
3. Clear sky statistics are compiled for each pixel using all clear values within some distance of the pixel and over some number of days (typically 150x150 km cells and 5 days). Medians of the channels 1 and 3 reflectances (day only) and the channel 4 temperature (day and night) are computed. If a cell occurs along a coastline, only pixels with the same surface type (LAND or NOT-LAND) as the center pixel are used. Pixels in the clear sky composite that did not have medians assigned due to the lack of clear values are filled with a kriging interpolation scheme. The probability of finding clear pixels can be increased by enlarging the cell size or using more days, but doing so also increases the variability and may adversely affect the next step.
4. The clear sky composite statistics are used in a final threshold operation to label or relabel all pixels as clear or cloudy. A pixel can be labeled as cloudy if its brightness temperature is higher or lower than its mean clear value plus or minus, respectively, some value that reflects the natural variability for clear sky, or if its reflectance in either channel 1 or 3 (daytime) is higher than its mean clear reflectance plus (not minus) some value (DEL\* in Table 3). However, the single-image spectral tests are run again in cloud-conservative mode and those pixels labelled as cloudy will also be cloudy in the final mask. This implies higher confidence in the spectral tests (with cloud-conservative thresholds) than in the final thresholding operation.

This scheme can be tuned by modifying the following: (1) single-image cloud mask spectral cloud test thresholds (file **cldmask1.pro**, (2) *ndays* (number of days in the clear sky compositing), *cellrad* (radius of cells for clear statistics), *MINCLEAR* (minimum number of clear values needed for statistics in a

cell), and *threshadj* in the calls to **cloudmask\_1** (procedures **cloudmask\_n** and **final\_threshold**); *ndays* and *cellrad* most directly control the number of values that go into the clear sky statistics, (3) time thresholds (procedure **clear\_pairs**), and (4) standard deviations multipliers (procedure **final\_threshold**).

Cloud masks for images at the beginning and end of the time series have a much larger uncertainty than those at least *ndays/2* places away from the ends. This results from the first and last few images being at the beginning or end of the *ndays* images on which the clear sky statistics were based. For example, given *ndays* = 5, the cloud mask for the first image is determined from the final thresholding based on clear sky statistics over days 1-5. The cloud mask for the third image is based on statistics from the same period. Obviously, the statistics are more representative of the third image of the first.

*Table 3.* Time and final thresholds used in cloud detection.

Threshold Variable	Value
TIMETHRESH3A	0.06
TIMETHRESH3B	0.04
TIMETHRESH1	0.07
TIMETHRESH4_LAND	3.0
TIMETHRESH4_OCEAN	2.0
TIMETHRESH45_LAND	0.40
TIMETHRESH45_OCEAN	0.35
DEL4LO_OCEAN	3.0
DEL4HI_OCEAN	3.0
DEL4LO_LAND	4.0
DEL4HI_LAND	4.0
DEL4LO_SNOW	6.0
DEL4HI_SNOW	6.0
DEL1	0.07
DEL3A_OCEAN	0.06
DEL3A_LAND	0.08
DEL3B_OCEAN	0.045
DEL3B_LAND	0.055

## CLOUD PARTICLE PHASE



This section describes the algorithms used in the determination of cloud particle phase. In CASPR, all clouds are composed of either liquid droplets ("water cloud") or solid ice crystals ("ice cloud"). No attempt is made to identify mixed-phase or multilayer clouds. The theoretical background for these procedures is detailed in Key and Intrieri (2000). Only a partial description is given here.

The determination of cloud particle phase, liquid or solid (generally referred to as "water" and "ice"), is based on both physical and spectral properties. Physically, liquid cloud droplets can exist at temperatures as low as -40 C, perhaps even lower, although clouds are likely to be composed of both liquid droplets and ice crystals at temperatures below -10 C. The spectral difference between water and ice clouds occurs because of differences in absorption and scattering. Based only on the imaginary index of refraction, which is an indicator of absorption, more absorption will take place in ice clouds at 11 and 12  $\mu\text{m}$  than in water clouds, so brightness temperature differences between 3.7 and 11 or 12  $\mu\text{m}$  will be larger for ice clouds. However, absorption alone does not provide enough information to explain observed spectral differences. The single scattering albedo indicates how effective a volume of particles are at scattering incident radiation. Unlike the imaginary index of refraction, it applies to size distribution of particles. Scattering is greater at 3.7  $\mu\text{m}$  than at 11 or 12  $\mu\text{m}$  and the smaller the particle, the greater the scattering. But for typical ice crystals sizes there is very little difference in scattering across this portion of the spectrum. Furthermore, the single scattering albedo indicates that during the day, ice clouds will exhibit a lower reflectance at 3.7  $\mu\text{m}$  than water droplets. At visible wavelengths, the single scattering albedo of both water and ice clouds is near unity and absorption is near zero.

For optically thick clouds, where the transmittance is near zero and the surface contribution to upwelling radiance is small, absorption and scattering define the spectral characteristics of a cloud. We expect the brightness temperature difference between channels 3 and 4 (BTD34) to be negative for water clouds with small effective radii. For thick ice clouds with particle effective radii of 30  $\mu\text{m}$  or larger, the single scattering albedo indicates that BTD34 would be near zero. This is, in fact, the case, as demonstrated by the model calculations (*Streamer*) presented in Figure 7. Both plots show that for visible optical depths  $\tau$  greater than 5, water cloud BTD34 is negative while ice cloud differences tend to be positive, at least for smaller water droplets and larger ice crystals. For larger optical depths BTD34 for ice clouds decreases. For optically thin clouds the transmissivity is not negligible and the surface temperature influences the brightness temperature measured at the satellite. BTD34 for cold water clouds (surface is warmer than the cloud) is positive when the optical depth is small. BTD34 for ice clouds takes on larger positive values in these cases. The opposite occurs for warm ice clouds, where BTD34 is negative.

The brightness temperature difference between 11 and 12  $\mu\text{m}$ , BTD45, is much smaller than BTD34 for both water and ice clouds, and there is considerable overlap in BTD45 for the two phases (Figure 8). The absolute value of BTD45 increases as cloud optical depth decreases (not shown). Therefore, large BTD45 differences (positive or negative) indicate thin clouds.

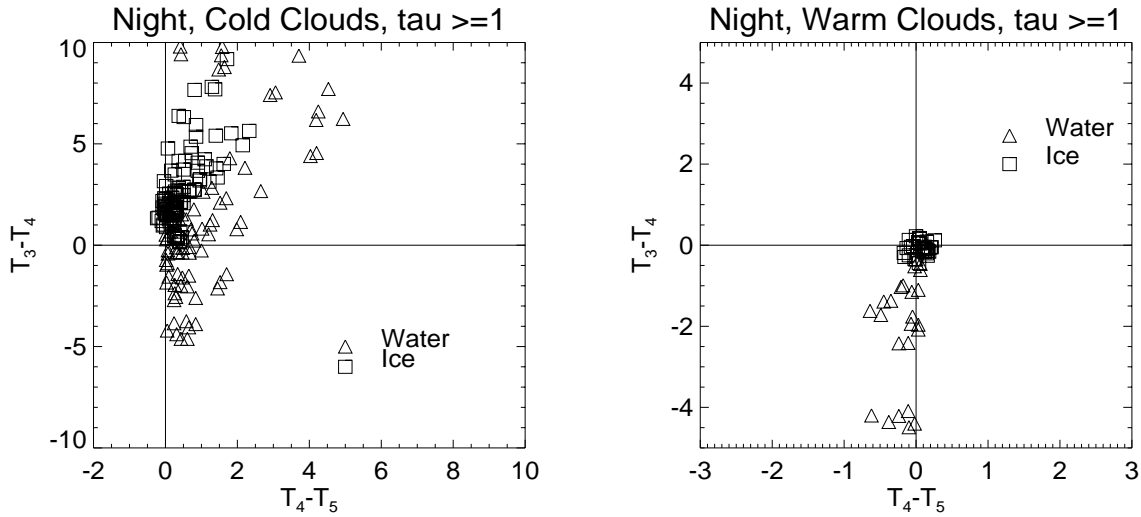


Figure 8. Modeled brightness temperature differences for AVHRR channels 3 minus 4 (3.7 minus 11  $\mu\text{m}$ ) and channels 4 minus 5 (11 minus 12  $\mu\text{m}$ ) for water and ice clouds. The visible optical depth for the data shown is one or greater. Water clouds have top temperatures greater than 250 K; ice clouds are less than 270 K. Calculations were done for tropical, midlatitude, and arctic conditions.

In the presence of solar radiation, the single scattering albedo at 3.7 or 1.6  $\mu\text{m}$  is the primary spectral feature used in distinguishing ice and water cloud. Ice particles do not scatter as efficiently as water droplets at this wavelength, due to both their indices of refraction (the real part) and the fact that ice clouds are typically composed of larger particles, which scatter less efficiently, than water clouds. However, the actual reflectance depends not only on particle phase, but also on viewing and illumination geometry and surface reflectance. This is illustrated in Figure 9, which shows the 3.7  $\mu\text{m}$  (NOAA-15 and earlier) and 1.6  $\mu\text{m}$  (NOAA-16 and later) modeled reflectances as a function of the scattering angle. The scattering angle  $\psi$  is the angle between the incident and reflected beams:

$$\psi = 180 - \text{acos}(\cos\theta_{sun} \cos\theta_{sat} + \sin\theta_{sun} \sin\theta_{sat} \cos\phi) \quad (15)$$

where  $\theta_{sun}$  is the solar zenith angle,  $\theta_{sat}$  is the satellite zenith angle, and  $\phi$  is the relative azimuth angle (where 0 is looking away from the sun and 180 is looking into the sun); all angles are in degrees. A scattering angle of  $0^\circ$  implies forward scattering;  $180^\circ$  means backscattering. The figure gives reflectances for cloud visible optical depths between 2 and 5, and for snow and vegetation surfaces. These two surface types exhibit somewhat different 3.7  $\mu\text{m}$  clear sky reflectances and very different clear sky reflectances at 1.6  $\mu\text{m}$ . However, their effect on the reflectance of thick clouds is minimal. The smooth curves represent approximate upper limits for ice cloud reflectance at each wavelength, valid for  $\psi$  values between  $0^\circ$  and  $160^\circ$  and for optically thick clouds. In the case of strong backscattering ( $\psi > 160^\circ$ ), and in the case of thin clouds, the separation between water and ice cloud is less clear.

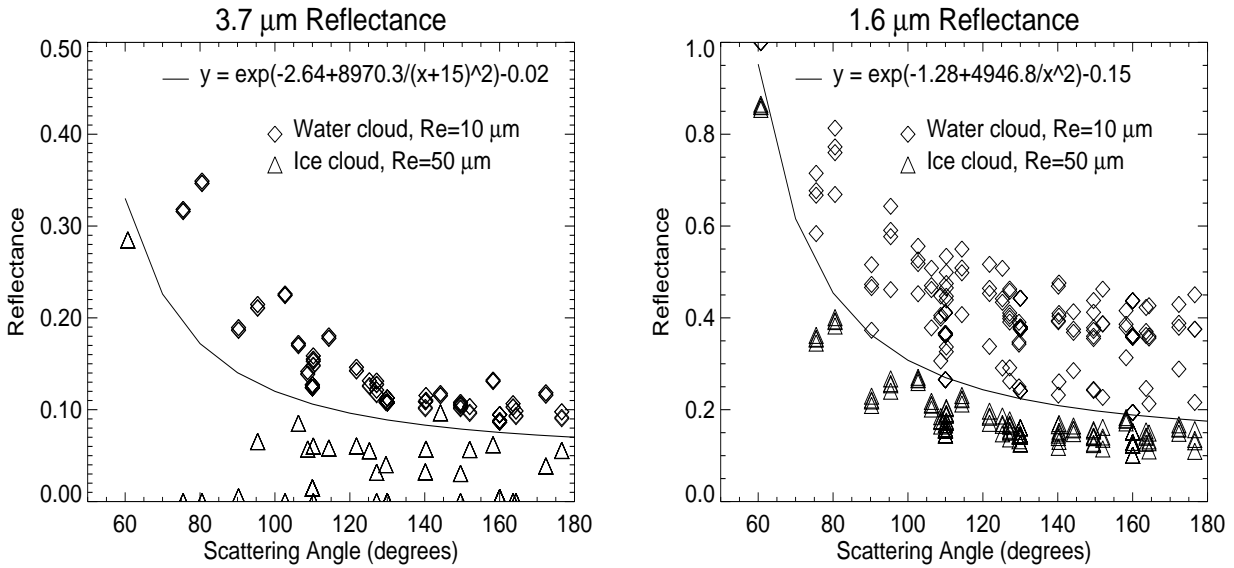


Figure 9. AVHRR channels 3 (3.7  $\mu\text{m}$ ) and 3A (1.6  $\mu\text{m}$ ) modeled reflectances as a function of scattering angle for water (diamond) and ice (triangle) clouds. All clouds have visible optical depths in the range 5-10. Also shown are the functions that approximately divide water and ice clouds at each of the two wavelengths. Calculations were done using midlatitude summer conditions.

## Procedures

The phase algorithm starts by exploiting the physical property that only ice crystals will exist below some threshold temperature and only liquid droplets will exist above some other threshold temperature. For optically thick clouds the 11  $\mu\text{m}$  brightness temperature will be very close to the kinetic temperature and simple temperature thresholds can be used to distinguish particle phase. For example, if  $T_4$  were less than some minimum value,  $\gamma_{\text{min}} = 243 \text{ K}$  (-30 C), then an optically thick cloud would almost certainly be composed of ice crystals. Similarly, if  $T_4$  were greater than some maximum value,  $\gamma_{\text{max}} = 273 \text{ K}$  (0 C) then the cloud would be liquid. But for optically thin clouds surface emission is a significant part of the measured radiance, and the relationship between the surface temperature and  $T_4$  must be considered. Using the two thresholds above there are four relationships between the surface temperature  $T_s$  and  $T_4$  that can be exploited to determine the phase, as listed in Table 4.

Table 4. Phase assignment based on temperature relationships.

Condition	Phase
$T_s - \delta < \gamma_{\text{max}}$ and $T_4 > \gamma_{\text{max}}$	Liquid
$T_s - \delta > \gamma_{\text{max}}$ and $T_4 > T_s$	Liquid
$T_s - \delta > \gamma_{\text{min}}$ and $T_4 < \gamma_{\text{min}}$	Ice
$T_s - \delta < \gamma_{\text{min}}$ and $T_4 < T_s$	Ice

The clear sky temperature can be used as a proxy for  $T_s$ , although  $T_s$  will generally be somewhat

lower than the clear sky value during the day (negative cloud radiative effect) and somewhat higher at night. The clear sky surface temperature can therefore be adjusted by a small amount  $\delta$ . At night  $\delta = -2$  K and during the day  $\delta = +2$  K in this study. The application of these four conditions constitutes the first step of phase determination. The tests in Table 4 do not handle water clouds with temperatures less than  $\gamma_{\max}$  or less than  $T_s$ , and ice clouds with temperatures greater than  $\gamma_{\min}$  or greater than  $T_s$ .

If no estimate of  $T_s$  is available then an alternate, though less robust, method would be to simply use simple thresholds; e.g., if  $T_4$  is less than 243 K (-30°C) then the cloud is ice and if  $T_4$  is greater than 303 K (+30°C) then the cloud is liquid. Hutchison et al. (1997) use -40°C for the lower threshold but suggest that -30°C is probably a reasonable lower bound. They do not suggest an upper bound for liquid clouds.

The second step employs the spectral properties described in the previous section and is different for day and night conditions. It is applied to the cloudy pixels that were not labeled in the first step. At night the tests are intended to identify optically thick ice cloud, thick water cloud, and most thin water cloud. The tests are: (a) if  $T_3 - T_4$  is less than -0.5 K then it is a water cloud and (b) if  $T_3 - T_4$  is greater than +1 K and  $T_4 - T_5$  is between 0 and 1 K then it is an ice cloud.

During the day the tests in the second step are based on the 3.7 or 1.6  $\mu\text{m}$  reflectance characteristics, utilizing the two reflectance functions shown in Figure 9. Only pixels with  $\psi$  less than 160 degrees and  $T_4 - T_5$  less than 1 K are evaluated, as reflectances for strong backscattering and thin clouds are ambiguous. Observed 3.7 or 1.6  $\mu\text{m}$  reflectances less than the threshold function values indicate ice cloud; those greater than the function values are water cloud.

The last step is to label any pixels that were not handled by the previous two steps. A simple temperature threshold is employed: if the 11  $\mu\text{m}$  brightness temperature is less than 258.16 K (-15°C) then the cloud phase is ice, otherwise it is liquid. Because of the low precision and high uncertainty in  $T_3$  (and therefore  $T_3 - T_4$ ) when temperatures are very low, all pixels with  $T_4$  less than 230 K are labelled as ice.

### ***Remaining Problems***

The procedure described here labels all cloudy pixels as either ice (solid) or water (liquid). Multi-layer and mixed-phase clouds are not identified as such. This problem is particularly apparent in the case of an ice cloud over a water cloud during the day. If the ice cloud is cold the temperature tests (step 1) will label it as ice. The reflectance test (step 2) will not relabel it even though its reflectance is high. Ice over water multilayer clouds that are not labeled by the temperature tests will be labeled as water clouds by the reflectance test. In both cases the result is not incorrect, but is not completely correct either.

Incorrect results typically occur in two other situations. Very thin water clouds over snow/ice may be mislabelled due to the low reflectance of the underlying surface. The same will be true of clouds that occupy only a small proportion of a pixel, as often occurs for cumuliform clouds and cloud edges.

## **CLOUD OPTICAL DEPTH AND PARTICLE EFFECTIVE RADIUS**

The retrieval of cloud optical and microphysical properties from the AVHRR or AVHRR-like wavelengths has a long history; only a sample of the literature is given here. Hunt (1973) demonstrated the sensitivity of cloud emittance to changes in optical depth and particle size at thermal wavelengths. Liou (1974) showed that cirrus optical properties varied between 11 and 12  $\mu\text{m}$ . Arking and Childs (1985) describe a technique for extracting a microphysical model parameter from AVHRR data. Inoue (1985) used the split-window channels to estimate cloud optical depth with an implicit particle size, while d'Entremont (1986) detected low clouds and fog at night using the variation of the 3.7-11  $\mu\text{m}$  difference with particle size. Using a radiative transfer model and ground-based lidar for validation, Stone et al. (1990) discuss the problem of retrieving cirrus cloud optical depth from radiance measurements. Lin and Coakley (1993) used AVHRR channels 4 and 5 to simultaneously solve for the emittance and cloud fraction. Ou et al. (1993) developed a method to derive optical depth, cloud top temperature, and effective

radius from nighttime observations in AVHRR channels 3 and 4. Baum et al. (1994) modeled brightness temperature differences for liquid and ice clouds over the ocean. A review of cloud observations using satellites is given by Rossow (1989).

The importance of cloud optical depth  $\tau$  and the particle effective radius  $r_e$  for remote sensing lies in the fact that the optical properties of clouds used in the calculation of radiative fluxes, the single scattering albedo, the asymmetry parameter, and the extinction coefficient, are proportional to the optical depth and effective radius. Cloud optical depth (unitless) is a measure of the cumulative depletion of radiation as it passes through the cloud. It is related to the transmissivity  $t$  via

$$t = e^{-\tau} \quad (16)$$

and is a product of the volume extinction coefficient and the physical thickness of the cloud.

The particle effective radius for liquid droplets is the ratio of the third to second moments of the drop size distribution  $n(r)$ :

$$r_e = \frac{\int_0^{\infty} r^3 n(r) dr}{\int_0^{\infty} r^2 n(r) dr} \quad (17)$$

For ice crystals the size parameter is better termed the "mean effective size". It is based on the parameterization of Fu and Liou (1993), which was developed from ray tracing calculations for scattering by randomly-oriented hexagonal crystals. The mean effective size is defined as:

$$D_e = \left( \int_{L_{min}}^{L_{max}} D^2 L n(L) dL \right) / \left( \int_{L_{min}}^{L_{max}} D L n(L) dL \right) \quad (18)$$

where  $D$  is the width of an ice crystal,  $L$  is the length,  $n(L)$  is the size distribution, and  $L_{min}$  and  $L_{max}$  are the minimum and maximum lengths of ice crystals, respectively. In CASPR, "effective radius" refers to these two size parameters.

Cloud optical depth retrievals are done using a comprehensive data base of modeled reflectances and brightness temperatures covering a wide range of surface and atmospheric conditions (Key, 1995). Figures 10 and 11 give a few examples of the modeled data used in the retrieval of cloud optical depth and particle effective radius.


The basic approach for daytime retrievals of water (liquid) cloud follows that of Nakajima and King (1990) as illustrated in Figure 10. In the presence of solar radiation the retrieval is done using the reflectance in channels 2 and 3 (or 3A for NOAA-16 and later). For ice clouds under solar illumination the channel 3 reflectance is so small that it is unreliable. So channels 4 and 5 are used to obtain a range of possible solutions and channel 2 is used to constrain the solution. A valid solution exists if the observed brightness temperatures and BTDs fall within the range of the modeled data. If no valid solution was found, MISSING values are assigned.

At solar zenith angles greater than about 75-80 degrees over bright surfaces, uncertainties in modeled radiances and in the calibration of AVHRR channels 1 and 2 are large. When the solar zenith angle is greater than 80 degrees but less than 90 degrees, and when the surface clear sky channel 2 reflectance is high, only channels 4 and 5 are used in the retrieval. Solutions are obtained for all cloud top temperatures in the modeled data, and the effective radius/optical depth pair for the lowest cloud (arbitrary) that had a valid solution is given as the result. If no valid solution was found, MISSING values are assigned. Figure 3 shows the latitudes and times of the year where solar zenith angles greater than 75 degrees are experienced.

For nighttime retrievals, brightness temperature differences for channels 3 (or 3B) and 4 and 4 and 5 are employed (Figure 11). Both methods are based on the fact that the optical properties of clouds are different at each of the wavelengths examined. All three thermal channels are used for both liquid or ice clouds. The lookup table of brightness temperature differences is constructed for three different cloud top heights: 850, 650, 500 mb for liquid clouds and 700, 500, and 300 mb for ice clouds. The retrieval is done for each cloud top in both thermal channel combinations (3, 4 and 4, 5). The solution is the channel 4, 5 retrieval where the difference between the retrievals from both channel pairs is smallest.

In the lookup table procedure, interpolation to the observed values of solar zenith angle (0-85 degrees), precipitable water (2987-29,879 g m<sup>-2</sup>), and surface visible albedo (daytime; 0.06-0.99) or temperature (nighttime; 228-283 K). Single values of aerosol optical depth (0.06) and total column ozone (325 Dobson units) are used in all cases. Bilinear interpolation is done between effective radius and optical depth value pairs in the lookup tables; i.e., between the four points of each polygon in Figures 10 and 11. Effective radii for liquid clouds are 2.5, 6, 10, 14, 20 μm and for ice clouds are 20, 40, 60, 90, 120 μm. Optical depth values are 0, 1, 2, 4, 10, 20, 50, 80, and 150, with a maximum nighttime value of 15 and an ice cloud maximum of 50. The optical depth maximum for ice clouds is a result of their relatively low water contents. All clouds are modeled as either water or ice, with no mixed-phase clouds or overlapping combinations. Of course, it is entirely possible to have a liquid cloud under an ice cloud with a total optical depth greater than 50. This possibility will be addressed in a future version of CASPR.

For the daytime retrievals the reflectance of the surface under the cloud is assumed to be known. Similarly, the surface temperature under the cloud is needed for the nighttime retrievals. Neither can be measured directly from the AVHRR so they must be estimated. The relationship between the clear and cloudy sky reflectances depends on the cloud optical depth, phase, and the particle size distribution, and the anisotropic and spectral reflectance characteristics of the surface. The cloudy sky surface temperature is related to the clear sky temperature through the cloud base temperature, the residence time of the cloud, and the turbulent fluxes. Given the complexity of these relationships, no attempt is made to relate clear and cloudy temperatures or reflectances. A kriging procedure is used to create relatively smooth surfaces from the existing clear sky reflectances and temperatures for each surface type in the image. These clear sky surfaces are used as proxies to the actual surface reflectance and temperature in the optical depth/effective radius retrievals. The effect of using the clear sky values in place of the cloudy sky values is probably minimal for the daytime retrievals. At night, however, the effect can be significant, generally resulting in a positive bias in optical depth (i.e., the optical depths are too large) because clear sky surface temperatures may be considerably lower than cloudy sky temperatures.

	<p><b>CAUTION</b></p> <p>Effective radius and optical depth retrievals for low sun (large solar zenith angle) conditions have a large uncertainty.</p>
---	--

## CLOUD WATER PATH

Cloud water path is not computed explicitly but a procedure is available (**cloudwp**) in CASPR. Water path is calculated by converting the optical depth to a geometrical cloud thickness then multiplying it by the the cloud water content:

$$WP = z \cdot WC = \frac{\tau}{\beta} WC \quad (19)$$

where  $WP$  is the water path ( $\text{g m}^{-2}$ ),  $WC$  is the cloud water content or density ( $\text{g m}^{-3}$ ),  $\tau$  is the visible optical depth (unitless), and  $\beta$  is the volume extinction coefficient ( $\text{m}^{-1}$ ). For a homogenous cloud  $\tau = \beta z$ . The value for water content is the same as that used in radiative transfer calculations for the optical depth/particle effective radius retrievals:  $0.2 \text{ g m}^{-2}$  for water (liquid) clouds and  $0.07 \text{ g m}^{-2}$  for ice clouds. The extinction coefficient is also the same as that used in the radiative transfer calculations and depends on the particle effective radius.

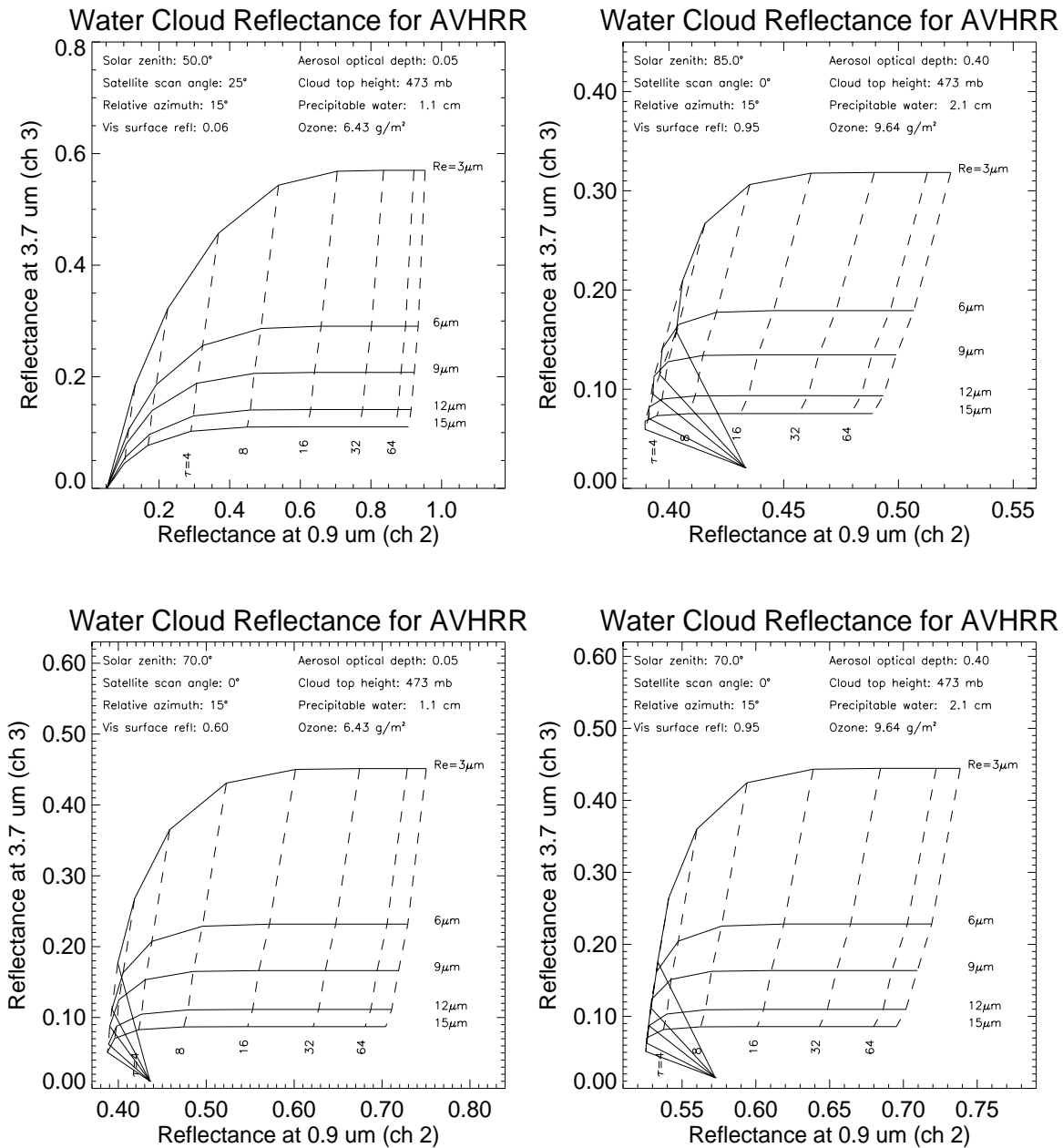


Figure 10. The relationship between two AVHRR reflective channels (2 and 3) as a function of water cloud optical depth and droplet effective radius over different surface types.

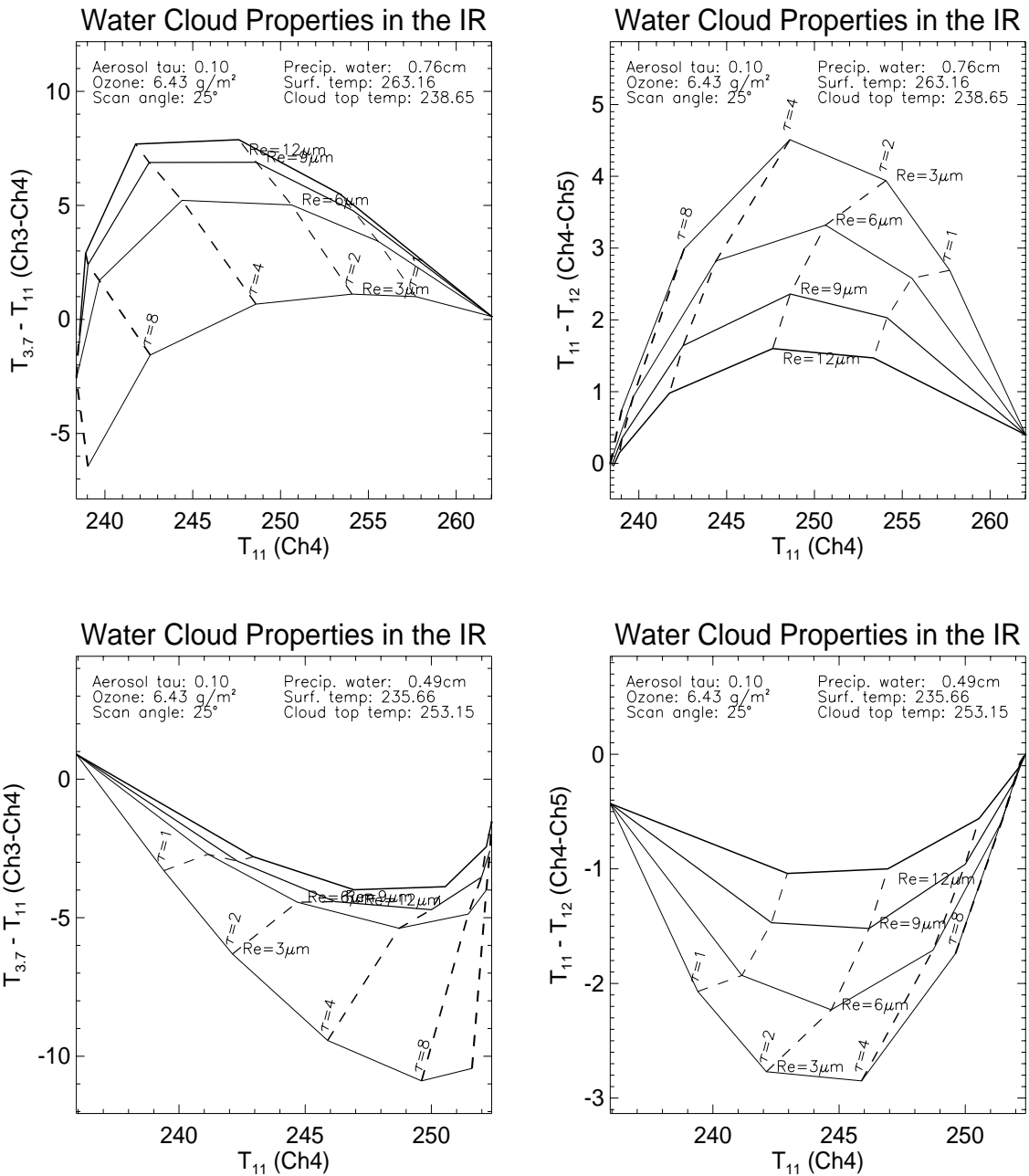


Figure 11. The relationship between the AVHRR channel 4 brightness temperature and the channels 4-5 difference as a function of water cloud optical depth and effective radius.



## CLOUD TEMPERATURE AND PRESSURE

The cloud temperature is determined from the channel 4 brightness temperature, the clear sky brightness temperature (not corrected for the atmosphere), and the visible cloud optical depth. The infrared optical depth is determined from the visible optical depth using the parameterizations of cloud optical properties in (12). The thermal cloud optical depth, which in the retrieval is a nadir (vertical) optical depth, is converted to an optical depth along the slant (viewing) path by dividing it by the cosine of the sensor scan angle. If this adjusted cloud optical depth is less than some threshold, the brightness temperature is assumed to be a function of both the cloud temperature and the upwelling radiation from the surface and atmosphere below the cloud. The threshold is taken from the ISCCP processing scheme, chosen such that clouds with optical depths greater than the threshold have transmittances of less than 1% (equivalent to an optical depth of 4.6) and are considered opaque. For opaque clouds the cloud top temperature is simply the channel 4 temperature. If the cloud is not opaque, then the cloud temperature is determined by first computing the cloud transmittance  $t$  from the infrared optical depth with (13), then calculating the cloud radiance that would be required to produce the observed radiance of the cloudy pixel, given the cloud optical thickness and the observed clear sky radiance (as an approximation of the surface radiance under the cloud):

$$L_c = \frac{L_4 - tL_{clear}}{1 - t} \quad (20)$$

where  $L_c$  is the cloud radiance,  $L_4$  is the channel 4 radiance, and  $L_{clear}$  is the clear sky radiance. If the estimated surface temperature is too low and the cloud is thin, then the cloud top temperature will be too high and vice versa. If the adjusted cloud top temperature is either lower than the tropopause temperature or higher than the maximum temperature from 950 mb to the tropopause, then it is reset to either the minimum or maximum temperature, as appropriate.

This scheme does not necessarily determine the cloud top temperature, but rather the effective radiating cloud temperature. While this may be close to the top temperature, it will generally represent a temperature somewhere beneath the cloud top. The differences between the retrieved cloud temperature and the actual cloud top temperature are illustrated in Figure 12 for two cases. For thin clouds the difference is greatest. Fortunately, the effect of this "error" on longwave radiative fluxes is small, because the thinner the cloud, the less is its influence.

The vertical location of the cloud, expressed as the cloud pressure, is determined by searching the temperature profile from the tropopause (or top of profile if below the tropopause) down. With this scheme, if a cloud has a temperature that could be either within or above an inversion, it will be placed below, i.e., closer to the surface (arbitrary). The physical thickness and cloud base height are determined from the cloud top height, the optical thickness, and an assumed cloud water content of  $0.2 \text{ g m}^{-3}$  for liquid clouds and  $0.07 \text{ g m}^{-3}$  for ice clouds.

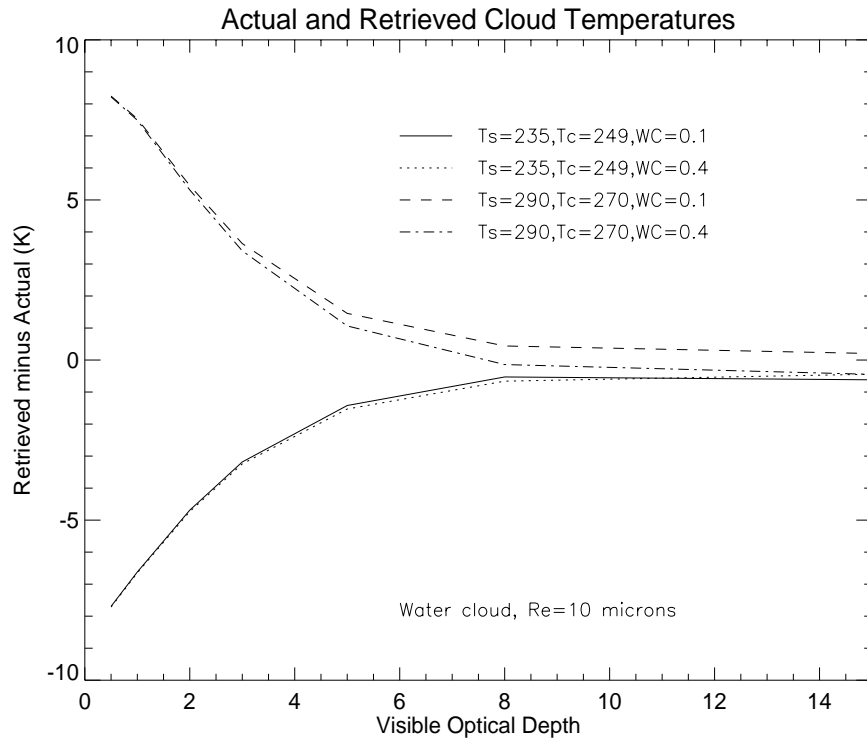



Figure 12. The difference between the retrieved cloud temperature and the actual cloud top temperature as a function of cloud optical depth. Differences are based on model simulations (Streamer) for two cloud-surface temperature relationships and for two cloud water contents ( $\text{g m}^{-3}$ ).

## 7. RADIATIVE FLUXES

Upwelling and downwelling shortwave and longwave fluxes at the surface are computed with a neural network trained to simulate a radiative transfer model. The neural network, called FluxNet (Key and Schweiger, 1998), is also available as a stand-alone program. The radiative transfer model that FluxNet is trained to simulate is Streamer Key and Schweiger, 1998). FluxNet v4.0 is used in CASPR. Relative differences between the neural network and the radiative transfer model for surface radiative fluxes are shown in Figure 13. Errors in top-of-atmosphere fluxes are similar. FluxNet is 100 to 10,000 times faster than Streamer, and is nearly as accurate. See the Web pages at <http://stratus.ssec.wisc.edu> for more information.



**CAUTION**  
*FluxNet* is very sensitive to out of range values.

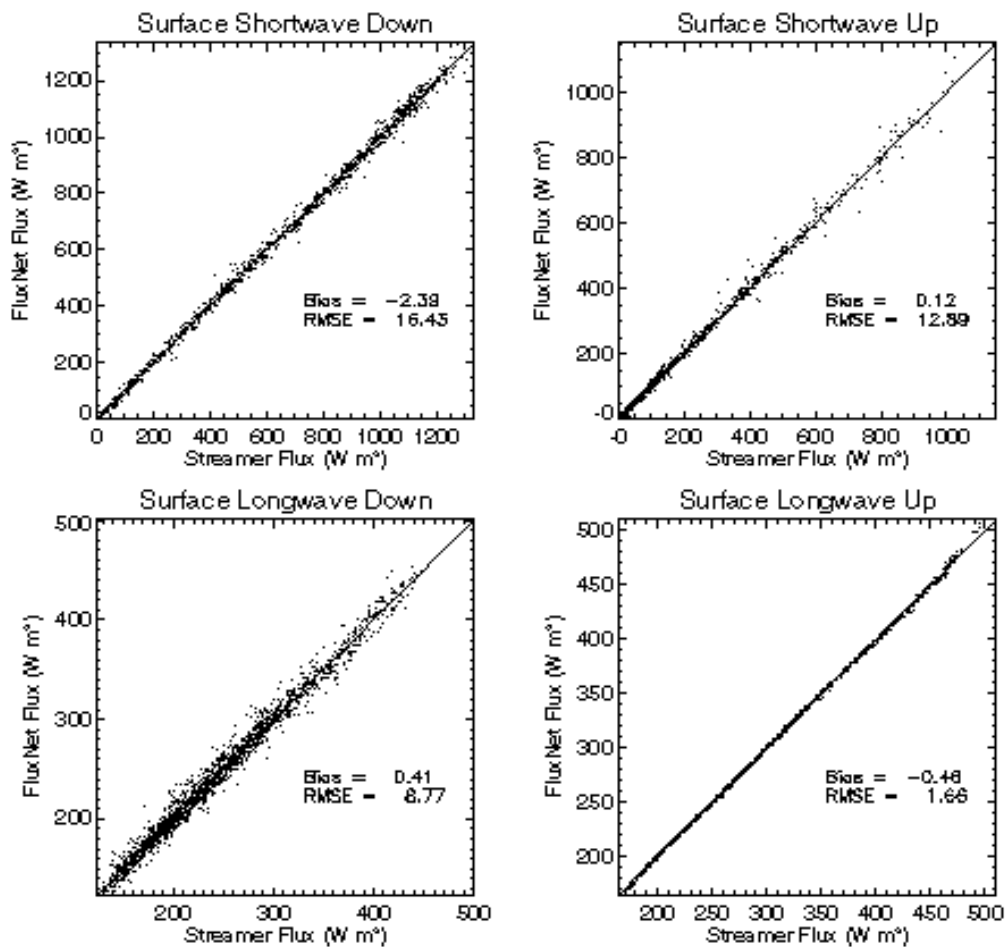


Figure 13. Comparison of FluxNet and Streamer fluxes for a wide range of atmospheric conditions.

The cloud radiative effect, more commonly called "cloud forcing", is computed from the net short-wave and longwave fluxes at the surface and TOA. It is defined as

$$CF_{\lambda, z} = \int_0^{A_c} \frac{\partial F_{\lambda, z}}{\partial a} da = F_{\lambda, z}(A_c) - F_{\lambda, z}(0) \quad (21)$$

where  $F_{\lambda, z}$  is the net flux ( $\text{W m}^{-2}$ ) for shortwave or longwave radiation ( $\lambda$ ) at the surface and  $A_c$  is the cloud fraction in the scene. The net flux is equal to the downwelling minus the upwelling fluxes. Because pixels are assumed to be either completely cloudy or completely clear, the right side of the equation is simply the net flux (shortwave or longwave) for a cloudy pixel minus the net flux if the pixel were clear. The clear sky net flux for cloudy pixels is calculated with FluxNet by simply setting the cloud fraction to zero and other cloud properties to values used in training FluxNet for clear sky conditions. Analogous to net radiation, the all-wave net cloud forcing can be calculated from

$$CF_z = CF_{shortwave} + CF_{longwave} \quad (22)$$

The net all-wave cloud forcing is not calculated in CASPR.

## 8. REFERENCES

---

- Allen, Jr., R.C., P.A. Durkee, and C.H. Wash, 1990, Snow/cloud discrimination with multispectral satellite measurements. *J. Appl. Meteorol.*, 29(10): 994-1004.
- Arking, A. and J.D. Childs, 1985, Retrieval of cloud cover parameters from multispectral satellite images, *J. Climate Appl. Meteorol.*, 24: 322-333.
- Baum, B.A., R.F. Arduini, B.A. Wielicki, P. Minnis, and S.-C. Tsay, 1994, Multilevel cloud retrieval using multispectral HIRS and AVHRR data: Nighttime oceanic analysis, *J. Geophys. Res.*, 99(D3): 5499-5514.
- Csiszar, I. and G. Gutman, 1999, Mapping global land surface albedo from NOAA AVHRR, *J. Geophys. Res.*, 104(D6), 6215-6228.
- d'Entremont, R.P., 1986, Low and mid-level cloud analysis using nighttime multispectral imagery, *J. Clim. Appl. Meteorol.*, 25: 1853-1869.
- DeAbreu, R.A., J. Key, J.A. Maslanik, M.C. Serreze, and E.F. LeDrew, 1994, Comparison of *in situ* and AVHRR-derived surface broadband albedo over Arctic sea ice. *Arctic*, 47(3): 288-297.
- Dozier, J. and S.G. Warren, 1982, Effect of viewing angle on the infrared brightness temperature of snow, *Water Resources Res.*, 18(5), 1424-1434.
- Ebert, E.E., 1987, A pattern recognition algorithm for distinguishing surface and cloud types in the polar regions, *J. Climate Appl. Meteorol.*, 26: 1412-1427.
- Ebert, E.E. and J.A. Curry, 1992, A parameterization of ice cloud optical properties for climate models, *J. Geophys. Res.*, 97(D4): 3831-3836.
- Fu, Q. and K.N. Liou, 1993, Parameterization of the radiative properties of cirrus clouds, *J. Atmos. Sci.*, 50(13), 2008-2025.
- Gustafson, G.B. et al., 1994, Support of Environmental Requirements for Cloud Analysis and Archive (SERCAA), Phillips Laboratory, Hanscom Air Force Base, Scientific Report No. 2, PL-TR-94-2114,; 100 pp.
- Hu, Y.X. and K. Stamnes, 1993, An accurate parameterization of the radiative properties of water clouds suitable for use in climate models, *J. Climate*, 6(4): 728-742.
- Hunt, G.E., 1973, Radiative properties of terrestrial clouds at visible and infra-red wavelengths, *Quart. J. Roy. Meteor. Soc.*, 99: 346-349.
- Inoue, T., 1985, On the temperature and effective emissivity determination of semitransparent cirrus clouds by bi-spectral measurements in the 10  $\mu\text{m}$  window region, *J. Meteorol. Soc. Japan*, 63: 88-99.
- Key, J., X. Wang, J. Stroeve, C. Fowler, 2001. Estimating the cloudy sky albedo of sea ice and snow from space. *J. Geophys. Res.*, in press.
- Key, J. and J. Intrieri, 2000, Cloud particle phase determination with the AVHRR, *J. Appl. Meteorol.*, 36(10), 1797-1805.
- Key, J. and A.J. Schweiger, 1998, Tools for atmospheric radiative transfer: Streamer and FluxNet. *Computers and Geosciences*, 24(5), 443-451.
- Key, J., A.J. Schweiger, and R.S. Stone, 1997, Expected uncertainty in satellite-derived estimates of the high-latitude surface radiation budget. *J. Geophys. Res.*, 102(C7), 15837-15847.

- Key, J., J. Collins, C. Fowler, and R.S. Stone, 1997, High-latitude surface temperature estimates from thermal satellite data, *Remote Sensing Environ.*, 61: 302-309.
- Key, J. and R.G. Barry, 1989, Cloud cover analysis with Arctic AVHRR, part 1: cloud detection, *J. Geophys. Res.*, 94 (D15): 18521-18535.
- Koepke, P., 1989, Removal of atmospheric effects from AVHRR albedos, *J. Appl. Meteorol.*, 28: 1341-1348.
- Li, Z. and L. Garand, 1994, Estimation of surface albedo from space: A parameterization for global application, *J. Geophys. Res.*, 99(D4), 8335-8350.
- Lin, X. and J.A. Coakley, Jr., 1993, Retrieval of properties for semitransparent clouds from multispectral infrared imagery data, *J. Geophys. Res.*, 98: 18501-18514.
- Lindsay, R.W. and D.A. Rothrock, 1994, Arctic sea ice albedo from AVHRR, *J. Climate*, 7(11): 1737-1749.
- Nakajima, T. and M.S. King, 1990, Determination of the optical thickness and effective particle radius of clouds from reflected solar radiation measurements. Part I: theory, *J. Atmos. Sci.*, 47(15): 1878-1893.
- NOAA, 1991, *NOAA Polar Orbiter Data User's Guide*, U.S. Dept. of Commerce., National. Ocean. and Atmos. Admin., NESDIS, February.
- Ou, S.C., K.N. Liou, W.M. Gooch, and Y. Takano, 1993, Remote sensing of cirrus cloud parameters using advanced very high resolution radiometer 3.7 and 10.9  $\mu\text{m}$  channels, *Appl. Opt.*, 32: 2171-2180.
- Rao, C.R.N., 1993, Degradation of the visible and near-infrared channels of the advanced very high resolution radiometer on the NOAA-9 spacecraft: assessment and recommendations for corrections. NOAA Technical Report NESDIS 70, U.S. Department of Commerce, 25 pp.
- Rossow, W.B., 1989, Measuring cloud properties from space: A review, *J. Climate*, 2: 201-213.
- Rossow, W.B. and L.C. Garder, 1993, Cloud detection using satellite measurements of infrared and visible radiances for ISCCP, *J. Climate*, 6(12): 2341-2369.
- Sakellariou, N.K., H.g. Leighton, and Z. Li, 1993, Identification of clear and cloudy pixels at high latitudes from AVHRR radiances, *Int. J. Remote Sensing*, 14(10): 2005-2024.
- Saunders, R.W. and K.T. Kriebel, 1988, An improved method for detecting clear sky and cloudy radiances from AVHRR data, *Int. J. Remote Sensing*, 9(1), 123-150.
- Stamnes, K., S.C. Tsay, W. Wiscombe and K. Jayaweera, 1988, Numerically stable algorithm for discrete-ordinate-method radiative transfer in multiple scattering and emitting layered media, *Appl. Opt.*, 27: 2502-2509.
- Stone, R.S., G.L. Stephens, C.M.R. Platt, and S. Banks, 1990, The remote sensing of thin cirrus cloud using satellites, lidar, and radiative transfer theory, *J. Appl. Meteorol.*, 29(5): 353-366.
- Stowe, L.L., E.P. McClain, R. Carey, P. Pellegrino, and G.G. Gutman, 1991, Global distribution of cloud cover derived from NOAA/AVHRR operational satellite data, *Adv. Space Res.*, 11(3), 51-54.
- Suttles, J.T., R.N. Green, P. Minnis, G.L. Smith, W.F. Staylor, B.A. Wielicki, I.J. Walker, D.F. Young, V.R. Taylor, and L.L. Stowe, 1988, Angular radiation models for Earth-Atmosphere system. Volume I-Shortwave radiation, *NASA Reference Publication 1184*, 144 pp.
- Taylor, V.R. and Stowe, L.L., 1984, Atlas of reflectance patterns for uniform earth and cloud surfaces (NIMBUS-7 ERB-61 days), NOAA Technical Report NESDIS 10, U.S. Department of Commerce, 66 pp.

- Toon, O.B. C.P. McKay, and T.P. Ackerman, 1989, Rapid calculation of radiative heating rates and photo-dissociation rates in inhomogeneous multiple scattering atmospheres, *J. Geophys. Res.*, 94(D13): 16287-16301.
- Tsay, S.-C., K. Stamnes and K. Jayaweera, 1989, Radiative energy budget in the cloudy and hazy Arctic. *J. Atmos. Sci.*, 46: 1002-1018.
- Welch, R.M., S.K. Sengupta, A.K. Goroch, P. Rabindra, N. Rangaraj, and M.S. Navar, 1992, Polar cloud and surface classification using AVHRR imagery: An intercomparison of methods, *J. Appl. Meteorol.*, 31: 405-420.
- Yamanouchi, T., K. Suzuki, and S. Kawaguchi, 1987, Detection of clouds in Antarctica from infrared multispectral data of AVHRR. *J. Meteorol. Soc. Japan*, 65(6): 949-961.

## 9. REVISION HISTORY

---

The table below lists the most important changes for each major version (vX.) and minor version (vX.Y). For bug fix releases (vX.Y.Z) and changes, see the detailed revision history at the web site.

Version	Date	Description
v4.0	18 Jan 2002	Added surface shortwave and longwave cloud forcing variables; added netCDF input/output procedures; added more NOAA-15 and -16 capabilities (surface temperature and cloud detection); updated to FluxNet v4; removed the requirement that radiative flux calculations require profiles; made low sun cloud optical depth retrievals more restrictive, and questionable particle size/optical depth retrievals are now set to missing (no data is better than bad data); rewrote the procedure to calculate cloud water path; more modifications to cloud masking, e.g., added the cloud cloud and clear tests; added the <i>full_landmask</i> keyword; added the capability to supply a different surface type mask for each image in a time series; rewrote the clear sky compositing, allowing for an input clear sky image; revised, as part of the clear compositing rewrite, the clear sky statistics procedures in <b>cloudmask_n</b> ; revised the daytime part of the cloud phase retrieval; updated the cloud optical depth lookup tables with results from Streamer v3.0; removed the dependence of aerosol optical depth input on location; numerous plotting changes including a revamping of image plotting; removed the calibration (channels 1 and 2) procedure; added procedures to extract values along a line of latitude or longitude.
v3.2	10 Feb 2001	Significant improvements to both single-image and time series masking; allows for a variable number of profile levels at each grid point; allows for a grid of total column ozone; allows for a "complete" surface mask (all surface types: LAND, OCEAN, ICE, and SNOW) to be input; some improvements to display procedures; new test images from the AVHRR Polar Pathfinder project; other minor changes.
v3.1	7 Feb 2000	Modified the single image cloud mask, particularly at night; added a clear sky "composite" for use with time series; redesigned the display procedures so that individual windows are used for each parameter;; renamed three procedures; updated the calibration coefficients and central wavenumbers and added NOAA 14; added NOAA 15 surface temperature support (other procedures for NOAA 15 are not implemented).
v3.0	27 Oct 1999	Redesigned surface albedo retrieval; upgraded FluxNet to v3.0 and added TOA fluxes; added cloudy sky surface temperature; changed optical depth retrieval for low sun angles; fixed bugs in cloud phase averaging.
v2.5	6 Apr 1999	Added computation of precipitable water from profiles; fixed major problem with <i>FluxNet</i> (that WC isn't really variable); fixed times series display problems.

---



---

v2.4	25 Feb 1999	Revised the cloud detection algorithms (thresholds and clear sky composites); changed re/tau interpolation for daytime liquid; added/modified some utilities .
v2.3	1 Jan 1999	Changed (refined) cloud particle phase algorithm.
v2.2	27 Aug 1998	Refined optical depth tables, fixed bugs.
v2.2B (beta)	5 Jul 1998	Added Earth-Sun distance correction; added type checking on IDL-C calls; improved cloud masking (single-image and time series); rewrote optical depth/effective radius retrieval.
v2.1B (beta)	20 Aug 1997	Redesigned neural networks to do only cloud optical depth and particle effective radius, and went back to original cloud temperature algorithm. Cleaned up the display procedures.
v2.0B (beta)	4 Aug 1997	Recoded many procedures to operate on arrays, some procedures are now in C; replaced the cloud tau, Re, Tc algorithm; eliminated the option to compute fluxes with Streamer; eliminated internal mean profiles; reduced the number of parameter categories, removed subsampling from caspr.

---

v1.11	1 Aug 1996	Implemented no_warn; fixed minor bugs.
v1.1	25 Jul 1996	Replaced parameterized flux scheme with FluxNet, added snow-free land surface temperature retrieval (v1.02), modified optical depth retrieval (v1.06).
v1.0	1 Jan 1996	Minor changes; much debugging.
v1.0A (alpha)	26 Jun 1995	First release.

---

